energies

MDPI

Article

Renewable-Energy-Powered Cellular Base-Stations in Kuwait's Rural Areas

Mohammed W. Baidas *, Mastoura F. Almusailem, Rashad M. Kamel and Sultan Sh. Alanzi

Department of Electrical Engineering, College of Engineering and Petroleum, Kuwait University, P.O. Box 5969, Safat, Kuwait City 13060, Kuwait; mastoura.almusailem@grad.ku.edu.kw (M.F.A.); rashad.mohammedeen@ku.edu.kw (R.M.K.); sultan.alanzi@ku.edu.kw (S.S.A.)
* Correspondence: m.baidas@ku.edu.kw

Abstract: Cellular network operators are actively expanding network coverage and capacity by deploying additional base-stations to provide mobile services to customers in rural areas. The increasing deployment of cellular base-stations has increased the power consumption, energy cost, and associated adverse environmental impact. This paper addresses the feasibility of using renewable energy sources to power off-grid rural 4G/5G cellular base-stations based on Kuwait's solar irradiance and wind potentials. More importantly, a hybrid renewable energy system will be designed and modeled to meet realistic energy demands of remote base-stations and determine the optimum size of the hybrid system components. Particularly, the hybrid off-grid system may incorporate wind turbines (WTs), photovoltaic (PV) solar panels, converters, a battery bank (BB), and a back-up diesel generator (DG). Two remote cell-sites are considered, namely: (1) Jal-Alayah and (2) Wafra, where the Jal-Alayah cell-site is characterized with higher average wind speed (and wind potential), while the Wafra cell-site has higher average clearness index and solar irradiance. Various hybrid PV/wind electric system (HPWES) configurations are modeled and simulated via HOMER software, with the aim of determining the optimal configuration—in terms of net present cost (NPC)—in each cell-site. Specifically, the simulations have revealed that the WT-BB configuration is the most economical at the Jal-Alayah cell-site while requiring minimal land area and ensuring 100% renewable energy and zero CO_2 emissions. This configuration is followed by the PV-DG-BB and PV-WT-DG-BB configurations, where the latter configuration incurs a marginal increase in the NPC than the former but with less land area. On the other hand, the PV-BB configuration is the most cost-effective in the Wafra cell-site; however, in the scenario of limited land area, then the PV-DG-BB configuration can be used but at the expense of slight increase in the NPC and CO_2 emissions. This study confirms that utilizing renewable energy sources in two rural areas in Kuwait can be extremely effective in replacing conventional DG-powered base-stations, while minimizing the NPC and CO_2 emissions.

Keywords: base-stations; cellular networks; HOMER; hybrid; off-grid; renewable energy; solar; wind

Citation: Baidas, M.W.; Almusailem, M.F.; Kamel, R.M.; Alanzi, S.S. Renewable-Energy-Powered Cellular Base-Stations in Kuwait's Rural Areas. *Energies* **2022**, *15*, 2334. https://doi.org/10.3390/en15072334

Academic Editor: Abu-Siada Ahmed

Received: 21 February 2022
Accepted: 22 March 2022
Published: 23 March 2022

1. Introduction

With the rapid development of mobile generations and cellular networks, wireless smart devices, services, and applications have reached new heights, with increasing subscriber demands. The evolution from the first generation (1G) to the fourth generation (4G), and more recently, with the fifth generation (5G) being rolled out worldwide, have continuously pushed the limits for higher data rates, spectrum-efficiency, low latency, broader coverage, and greater connection density [1]. This has led to an explosive increase in the number of mobile subscribers and data traffic, which resulted in base-stations (BSs) being increasingly deployed to provide coverage and ubiquitous communications. Consequently, the capital expenditure (CAPEX) and operational expenditure (OPEX) of cellular networks have increased significantly. Furthermore, the energy demand of cellular networks and the Information and Communication Technology (ICT) sector has drastically exacerbated,

with its carbon footprint surging to alarming rates [2], adversely affecting the environment and human health. It is well-known that cellular BSs are the largest power consumer in the network infrastructure, accounting for about 57% of the overall power consumption [3–5]. Additionally, most of today's BSs are operated via electrical grids or diesel generators (DGs), making cellular networks liable for the increasing carbon dioxide (CO_2) and greenhouse gas (GHG) emissions, globally. Thus, with the increase in energy cost and power consumption, an urgent need for "green communications" has arisen [6,7]. This, in turn, has prompted mobile network operators to pursue more innovative solutions to reduce energy consumption as well as dependency on electrical grids [8].

Powering cellular BSs via renewable energy sources (RESs) has attracted significant interest from academia and industry [9,10]. Solar photovoltaic (PV) and wind turbine (WT) power generation systems are the most prominent renewable solutions to power BSs, especially in rural and remote areas, where access to reliable electrical grids may not be available. Depending on the solar and wind potentials, combining the two different RESs could achieve higher reliability and efficiency compared to individual renewable sources [11]. As of 2020, more than 70,000 renewable-energy-powered BSs are in operation globally [12]. This is in alignment with the most telecommunication operators' objectives to use RESs to energize their BSs [13–16].

1.1. Related Works

Recently, several research works have considered the utilization of RESs to energize cellular networks. For instance, a hybrid PV/wind power system with a battery bank (BB) is proposed in [17] to reliably provide power to a remote cell-site in Ethiopia. Specifically, the PV-BB and PV-WT-BB system configurations have been evaluated using HOMER and compared to the conventional DG-BB system. Simulation results illustrated that the PV-BB configuration is optimal in terms of net present cost (NPC) and cost-of-energy (COE) (The NPC refers to the present value of all costs related to the installation and operation of a component/system minus the present value of all revenues earned over the project lifetime [18]. On the other hand, the COE is defined as the average cost per kWh of the useful electrical energy production of the system [19]). In [20,21], the authors focus on the long-term techno-economics of standalone solar-powered 4G cellular BSs in South Korea's urban locations using HOMER software. It has been shown that the PV-based energy system can significantly reduce the OPEX and NPC in comparison to DG-based systems while still meeting the BS load demand. The authors in [22] consider utilizing RESs to minimize the NPC and maximize the average energy savings of 4G BSs in Bangladesh. In particular, several electric system solutions—such as PV, PV-WT, PV-DG, and PV-Grid—are considered, with a focus on throughput, energy-efficiency, average energy savings, BS transmission power, and traffic intensity. It has been found that the PV-WT solution is the optimal in terms of COE, with zero GHG. In [23], a techno-economic and environmentally viable electric solution is presented for BSs in six locations in Nigeria. Various hybrid system configurations are compared in HOMER, where it is found that the PV-DG-BB configuration is optimal in terms of NPC, COE, renewable energy fraction (REF), and CO_2 emissions. Another study considered various locations in Nigeria [24], with the aim of finding the proper generator schedule and renewable energy system configuration to reduce OPEX. Specifically, it has been revealed that a 50% reduction in OPEX can be achieved in comparison to traditional DG-powered BSs, while reducing the Carbon footprint by 30 to 70%. The feasibility of using off-grid hybrid renewable energy systems in Pakistan is studied in [25], where it has been determined that the PV-WT-DG-BB system configuration yields the lowest NPC, COE, and CO_2 emissions. In [26], an off-grid PV-BB system is proposed and analyzed for powering BSs in Oman. It has been found that the proposed system yields lower NPC than conventional DG-based systems, while reducing OPEX by approximately 15.24%. The authors in [27] study the possibility of reducing OPEX and GHG emissions for rural BSs in Malaysia by utilizing a PV-DG-BB hybrid system. Using HOMER, it has been shown that an average annual OPEX saving of 43–47% is

achieved, while reducing CO_2 emissions. Since Malaysia is characterized by a tropical climate, the proposed system is applied to Germany, which is a four-season country. It has been revealed that Malaysia has higher potential for the proposed system, and achieves a lower NPC than in Germany. A summary of similar works in different countries can be found in [14].

1.2. Kuwait's Renewable Energy Prospects

Kuwait is located between 28° and 31° N and longitudes 46° and 49° E and extends over area of 17,818 km^2 [28]. The climate is characterized by two main seasons, a dry and hot summer and a short—relatively warm—winter [29]. Electricity peak demand in Kuwait has significantly increased from 10.9 GW in 2010 to 15.7 GW in 2021, and is projected to increase to over 22 GW by 2030 at an annual rate of 4% [30–32]. Figure 1 illustrates the actual and projected maximum peak load in the period from 2010–2030. Kuwait's energy needs are fulfilled through fossil-fuel-dependent (e.g., oil and natural gas) power plants, making them responsible for 95% of the country's total CO_2 emissions. Not only that, an annual per capita CO_2 equivalent to 21.6 tonnes makes Kuwait higher than the average of the world [33]. Currently, many new cities and residential areas are being built in Kuwait to meet the housing crisis [34], which will exacerbate the energy demands. Thus, reliance on non-renewable resources presents a challenge in the future.

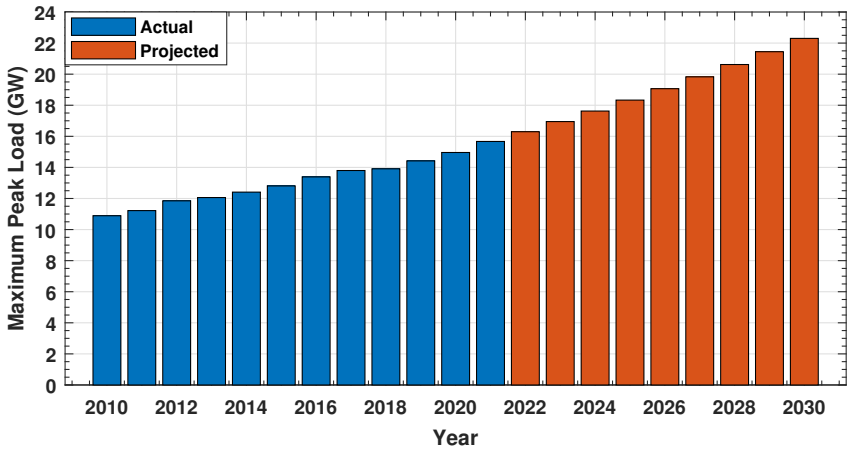

Figure 1. Actual and projected maximum peak load in Kuwait.

The rising and fluctuating price of fuel, associated costs, and harmful emissions have put immense pressure on cellular operators to supply electricity to BSs reliably and cost-effectively. Moreover, electrical grids are not typically available in remote locations, which is due to the fact that urbanized lands constitute no more than 10% of Kuwait's total area. Therefore, supplying power to BSs in rural areas is a significant challenge. Typically, DGs are used to supply electrical power to BSs in remote locations in Kuwait, which entails additional costs for the transfer of fuel as well as operation and maintenance (O&M). The resulting air pollution due to CO_2 and GHG emissions can be added to this. Thus, using DGs to power cellular BSs has become economically and environmentally less viable for cellular operators. Accordingly, the exploitation of RESs in the rural areas of Kuwait as a long-term solution is an ideal alternative to achieve green communications.

The predominant and abundant RESs in Kuwait take the form of solar and wind [35–37]. Kuwait's solar potential is estimated in terms of global horizontal irradiance (GHI) at 1900–2100 $kWh/m^2/year$ [38] (GHI represents the total solar radiation incident on a surface horizontal to the ground [39]), while the clearness index ranges between 55 and 70% [40]. The annual average wind speed ranges from 3.7–5.5 m/s with mean wind power density in the range 80–167 W/m^2 at standard height of 10 m [41]. Kuwait has stated a national goal of 15% renewable energy generation by 2030 and thus has established several projects. For instance, the Shagaya Renewable Energy Park (SREP) project comprises the generation

of 50 MW, 10 MW, and 10 MW from a concentrated solar power (CSP) plant, a PV plant, and a wind farm, respectively [42]. The Al-Dibdibah Solar Project is planned to provide over 3500 MW and is expected to yield a reduction of at least 2.1 million tons of CO_2 emissions per year [43]. Moreover, the electricity and water authorities aspire to provide 4500 MW of solar and wind capacity by 2030 [44]. Nevertheless, Kuwait has a long way to go to reduce its CO_2 emissions, as it is expected to emit more than four times the world's average of CO_2 emissions per capita in 2035 [43].

A number of studies have been conducted in Kuwait, on various aspects of RES development and utilization. In [41], a study of the potential wind power generation in eight sites in Kuwait is presented and showed that open flat areas are sufficient for power generation, since the wind power density and wind speed are high. Furthermore, the authors in [45] provided an overview of wind and solar energy resources in Kuwait, and proposed a strategy for potential uses of each renewable resource and raised awareness of using renewable resources as a supplement to conventional energy resources. In [31,36], the authors analyzed a wind power system's feasibility in six locations in Kuwait for electricity production and optimized the sizing in three sites for remote housing electrification to verify technical and economical features. Particularly, different wind turbine and storage battery sizings, the average cost in stand-alone and grid connection, and an assessment of wind energy characteristics have been presented and discussed. The benefits of using wind systems in Kuwait using a geographical spatial analysis has been studied in [37].

In Kuwait, the total number of mobile subscribers reached 6.77 million in 2020 (158.5 per 100 people) [46,47], distributed over 3 mobile operators, namely, Zain [48], Ooredoo [49], and STC [50], with over 1150 cellular BSs. Therefore, there is an urgent need to utilize renewable-energy-powered cellular BSs in Kuwait.

1.3. Motivations and Contributions

Due to the potentials of solar and wind in Kuwait, and to reduce dependency on the electrical grids and conventional DGs, the main goal is to design an off-grid hybrid PV/wind electric system (HPWES) that could serve as a cost-effective electric system to energize cellular BSs in rural areas in Kuwait, while potentially minimizing the use of DGs. This, in turn, could reduce (or completely eliminate) CO_2 emissions, which constitute a serious threat to the environment and health. Not only that, but utilizing an HPWES could reduce the NPC and COE over the system lifetime in comparison to conventional DG-based electric systems. In addition, PV/WT hybrid systems can greatly reduce costs associated with cell-site visits for repairs and re-fueling if DGs are used, especially in rural cell-sites. Specifically, the use of the DGs increases the technical problems and reduces efficiency, since 70% of the fuel energy is not converted to electricity [51] (In some cases, using DGs as back-up energy sources is necessary; however, this comes at the expense of reduced energy-efficiency, as well as increased cost and harmful emissions). Moreover, more than 65% of outages in cellular network services in rural areas are due to malfunctions in the DGs [27].

This paper focuses on the feasibility of utilizing RESs to power rural 4G/5G cellular BSs in Kuwait's rural areas. To meet the BS load demand, an off-grid HPWES will be designed, modeled, and optimized via HOMER software [52–54], with the aim of determining the optimal system configuration that minimizes the NPC. The system design and configuration may incorporate WTs, PV panels, converters, charge controllers, a battery bank (BB), and a back-up DG. Furthermore, two cell-site locations are considered, namely: (1) Jal-Alayah and (2) Wafra. In particular, the Jal-Alayah cell-site is characterized by a higher average wind speed (and wind potential), while the Wafra cell-site has a higher clearness index and average GHI. In turn, the PV panels and WTs must be carefully selected and optimized to meet realistic load demands at both cell-sites. Specifically, two PV panels and two WTs with different rated power values are considered at each cell. Extensive numerical results are presented to determine the optimal system configuration at each cell-site, with various combinations of WTs, PV, BB, and DG. In particular, it has been determined that the

WT-BB configuration is the most economical at the Jal-Alayah cell-site while requiring minimal land area and yielding zero CO_2 emissions and 100% renewable energy. This configuration is followed by the PV-DG-BB and PV-WT-DG-BB configurations, where the latter configuration incurs a negligible increase in the NPC than the former configuration but with less land area. At the Wafra cell-site, the PV-BB configuration yields the lowest NPC, however, at the expense of high land area. In the scenario of limited land area, the PV-DG-BB configuration can be considered, at the expense of a slight increase in the NPC and CO_2 emissions. This study confirms that RESs can be used to energize cellular BSs in Kuwait's rural areas, while reducing dependency on conventional DGs, and minimizing the NPC and CO_2 emissions. In general, the use of PV panels and WTs is location-dependent and mainly governed by the solar and wind potentials at each cell-site.

To the best of our knowledge, no prior work has considered renewable-energy-powered cellular BSs in Kuwait's rural areas. Thus, the main contributions of this paper are summarized as follows:

1. Studying the potentials of hybrid solar- and wind-powered BSs in two rural cell-sites in Kuwait, based on realistic 4G/5G base-station load profiles;
2. Modeling and analyzing the off-grid HPWES components based on realistic economic factors, various system configurations, and different PV panels and WTs;
3. Simulating various electric generation systems for two rural cell-site locations to gain more insights into the potentials of renewable energy at each cell-site, while focusing on NPC-minimizing optimal system sizing;
4. Presenting extensive numerical results and comparisons for various system configurations for two remote cell-sites from the perspective of NPC, fuel consumption, CO_2 emissions, and required land area;
5. Demonstrating that the WT-BB configuration is optimal at the Jal-Alayah cell-site in terms of NPC, required land, and CO_2 emissions, while the PV-BB configuration is optimal at the Wafra cell-site in terms of NPC and CO_2 emissions but at the expense of high land area.

This work provides a platform to the development and deployment of practical green sustainable cellular BSs in Kuwait's rural areas, while eliminating the dependency on the electrical grid. Lastly, it should be noted that our previous work has focused on a solar-powered cellular BS in a densely populated urban city, close to the capital city of Kuwait [55]. It has been revealed that the PV-DG-BB configuration yields the lowest NPC, while reducing fuel consumption by almost 95% in comparison to conventional DG-powered BSs.

The rest of this paper is organized as follows. Section 2 details the problem definition, modeling, and workflow. The proposed off-grid HPWES design is outlined in Section 3, whereas the simulation set-up and techno-economic specifications are presented in Section 4. Section 5 presents the simulation results, whereas the conclusions are drawn in Section 6.

2. Problem Definition, Modeling, and Workflow

2.1. Problem Definition

The aim of this paper is to study the potentials of utilizing hybrid RESs to design an off-grid electric system that energizes cellular BSs in Kuwait's rural areas. To gain a comprehensive picture, two cell-site locations—with different average wind speed, clearness indices, and GHI characteristics—will be considered, namely: (1) Jal-Alayah and (2) Wafra. This entails data collection of realistic solar and wind data and BSs' load profiles and components selection, along with their technical and economic specifications. This is followed by system modeling and design, which entail the consideration of various system configurations, appropriate cost modeling, and performance criteria. After that, the different system configurations are simulated in HOMER with the goal of minimizing the NPC to meet the load demand of the BSs at the two cell-sites. More importantly, the simulation results will be presented in terms of the system components, COE, NPC,

REF, fuel consumption, and CO_2 emissions. Lastly, the obtained results will be contrasted at both cell-sites.

2.2. Modeling and Workflow

Based on the problem definition, an off-grid HPWES must be designed to meet the BS load demand at each cell-site. This entails two main tasks: (1) cell-site selection and (2) Pre-HOMER modeling, which are then amalgamated to determine the optimal HPWES system design and performance criteria. For the first task, two BS cell-sites with different solar and wind data characteristics must be carefully selected, along with their AC/DC BS load profiles. On the other hand, and to realistically model the HPWES (i.e., in the Pre-HOMER modeling task), the system specifications (e.g., technical constraints), system economics (i.e., cost model and project lifetime), and component technical and economic specifications must be defined. This is followed by system design and modeling for various system configurations (based on PV panels, WTs, DG, and batteries). After that, the system design along with the BS load profile as well as the solar/wind data at each cell-site are incorporated into HOMER to obtain the techno-economic results. Specifically, the optimal system sizing, cost factors, and resulting fuel consumption and CO_2 emissions are obtained. Lastly, a detailed discussion of results will be presented, and conclusions will be drawn. The considered workflow is demonstrated in Figure 2.

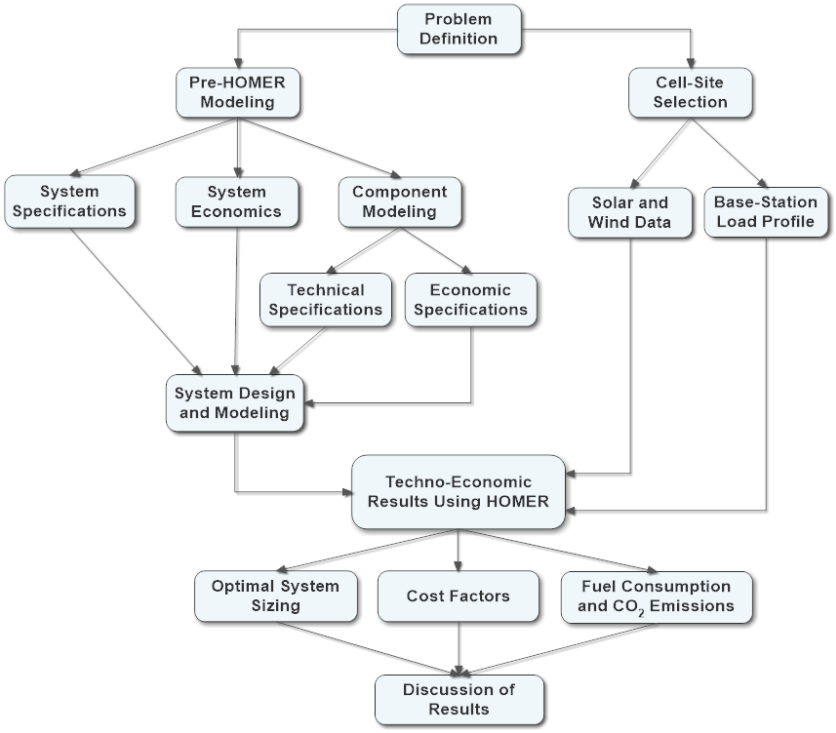

Figure 2. Modeling and workflow.

3. System Model and Design

Figure 3 illustrates the proposed HPWES design, which comprises the BS load (i.e., AC and DC loads) and the electrical power system (i.e., PV panels, WTs, DG, BB, converters, etc.). The system components can be described as follows:

1. PV Panels: The PV panels absorb the sunlight and convert it into DC electricity, thus providing power to the DC load of the BS and charging the batteries.
2. Wind Turbines: The wind turbines convert the kinetic energy of wind into mechanical energy, which is then converted into electrical energy. The main WT components are the gearbox, nacelle, electrical generator, rotor hub, rotor blades, and the tower [56,57]. For safety and protection, hydraulic brakes, a pitch controller, and a yaw controller on

a nacelle are used. The pitch power controller is an automatic controller for turbine output power. If the output power level exceeds the rated level, it sends a signal to turn the blades out of the wind to stabilize the output power. However, at low power levels, the blades are pitched back to catch the wind at an optimal angle to ensure maximum power output.

3. Battery Bank: The battery bank is charged in normal operation cases to be used during periods of insufficient energy, and peak load demand. This may occur when the PV panels and/or WTs malfunction, and thus the BB provides energy to the BS load before reaching the maximum depth-of-discharge (DoD).
4. Dump Load: The dump load box is used in some turbines in the case of an over-voltage fault, which is to keep the power output stable, and control the peak voltage with pitch control. Particularly, the dump load is a resistor that diverts electricity from the BB once it is fully charged, even when the WTs are still generating power, where excess electricity is converted into heat. Most modern WTs incorporate built-in dump load controllers.
5. Wind Solar Hybrid Controller: The hybrid charge controller is used to regulate the energy before delivering it to the battery, so as to prevent overcharging, overheating, and deep discharging of the battery [14].
6. Converter: Various types of converters are used to convert the DC voltage from the PV panels and battery into usable AC voltage, and the AC voltage from the WTs and DG into DC voltage. Moreover, the DC/DC converter is used to convert a DC voltage from one level to another.
7. Diesel Generator: The DG is used as a back-up energy source if the BB is not sufficient to cover the load peak demand.
8. Control Unit (CU): The CU manages the flow of power from the power sources and storage devices (i.e., PV panels, WTs, BB, and DG) to meet the BS load demand and avoid power outages to the BS. Moreover, the CU incorporates a dispatch strategy, which determines how and when batteries are charged/discharged, and the priority with which the energy is supplied to meet the load demand (In Figure 3, the green dashed line represents the control signal between the control unit, hybrid controller, battery bank, and diesel generator).

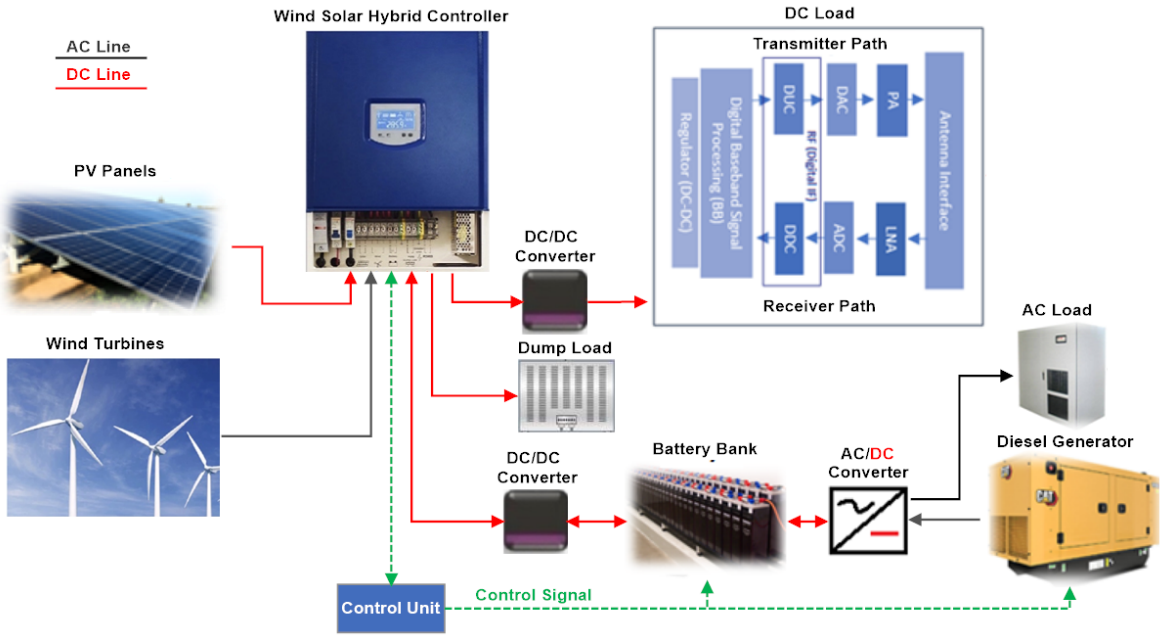

Figure 3. Schematic of the proposed hybrid PV/wind electric system.

In the proposed HPWES system design, the PV panels and WT provide power to the BS. However, in the case of insufficient power by the PV panels and/or WTs, the BB

provides power to the BS. Moreover, if the BB cannot provide sufficient power to the BS, or has already reached its maximum DoD, the DG (as a back-up source) is operated to provide the necessary power to the BS to ensure the continuity of BS operation.

4. Simulation Set-Up and Techno-Economic Specifications

4.1. System Configurations

In the simulations, eight off-grid system configurations are considered in HOMER:

1. PV-WT-Battery Bank (PV-WT-BB);
2. PV-DG-Battery Bank (PV-DG-BB);
3. WT-DG-Battery Bank (WT-DG-BB);
4. PV-WT-DG-Battery Bank (PV-WT-DG-BB);
5. PV-Battery Bank (PV-BB);
6. WT-Battery Bank (WT-BB);
7. DG-Battery Bank (DG-BB);
8. DG-Without Battery Bank (DG-WBB).

Particularly, in HOMER, the above system configurations will be optimized to meet the BS load demand while simultaneously minimizing the NPC. In the system configurations, two PV panels and two WTs are compared (i.e., a total of four cases per cell-site). Specifically, the PV panels are [58,59]:

1. CS6K-285 (285 W);
2. SunPower475 (475 W),

while the considered WTs are [60,61]:

1. Bergey Excel XL10 (10 kW);
2. Eocycle EO20 (20 kW).

It is noteworthy that conventional BSs utilize the DG-BB and DG-WBB configurations. Particularly, the former configuration utilizes the BB to power the BS in the case when the DG runs out of fuel or malfunctions. On the other hand, the DG-WBB leads to a network coverage outage if the DG is not operational, which is due to the absence of the BB.

The simulated system model in HOMER is depicted in Figure 4, which is based on the system design presented in Figure 3. Specifically, Figure 4 represents the main system components that will be optimized to meet the AC/DC loads of the base-stations based on aforementioned system configurations. The techno-economic specifications of the system components, as well as the solar and wind data and BSs' load profiles at the considered cell-sites will be incorporated into HOMER to determine the optimal system sizing and several performance criteria.

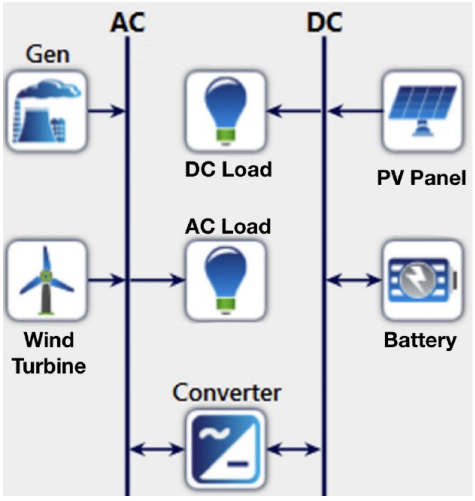

Figure 4. Simulated system model in HOMER.

4.2. Cell-Sites

Two cell-site locations are considered in this work to gain insights into the potentials of solar and wind energy in the rural areas of Kuwait. Specifically, cell-sites at (1) Jal-Alayah and (2) Wafra are considered, as shown in Figure 5. The Jal-Alayah cell-site is located North West the capital city of Kuwait (longitude 47.678° E and latitude 29.609° N), while the Wafra cell-site is located south of the capital city of Kuwait (longitude 48.203° E and latitude 28.695° N).

Figure 5. Two considered rural cell-site locations in Kuwait.

It should be noted that HOMER utilizes the NASA Prediction of World Energy Resource (POWER) database [40], where the average wind speeds for Wafra and Jal-Alayah have been obtained at 50 m above the surface of Earth over a 30 year period. In HOMER, the wind speed profile follows a power law, with a power law exponent equal to 0.14. In this work, the two-parameter Weibull distribution is used to model the wind speed V_w, where the probability density function (PDF) is given by [62]:

$$f_{V_w}(v) = \frac{\kappa}{c}\left(\frac{v}{c}\right)^{\kappa-1} e^{-\left(\frac{v}{c}\right)^{\kappa}}, \tag{1}$$

where v is the value of the wind speed, k is the shape factor, and c is a scaling parameter. Moreover, the average wind speed is related to the Weibull parameters as:

$$\bar{v} = c\Gamma\left(\frac{1}{\kappa}+1\right), \tag{2}$$

where $\Gamma(\cdot)$ is the Gamma function [63]. In [41], the wind power density based on the Weibull function parameters has been estimated based on six stations, distributed in different parts of Kuwait. However, the considered cell-site locations in Jal-Alayah and Wafra are different from the stations' locations considered in [41]. This is in addition to the different recorded monthly average wind speeds over 30 years, which is due to the atmospheric and structural changes. Thus, the interpolation method has used to obtain the value of the shape factor κ. Specifically, the Jal-Alayah and Wafra average wind speeds have been calculated using:

$$\frac{V_w(h)}{V_w\left(h_{ref}\right)} = \left(\frac{h}{h_{ref}}\right)^{\alpha}, \tag{3}$$

in which $V_w(h)$ is the wind speed at height h above ground "reference" level h_{ref}. Moreover, $0.05 \leq \alpha \leq 0.5$ is the the surface roughness factor, and is usually set as $\frac{1}{7} \approx 0.14285$ for Kuwait [64]. At an anemometer height of 10 m, the wind speed in Jal-Alayah and Wafra cell-sites have been calculated as 4.93 m/s and 4.74 m/s, respectively. Accordingly, the shape factors κ are set to 2.24 and 2.09 for Jal-Alayah and Wafra, respectively. In the simulations, the height above sea level in Jal-Alayah and Wafra cell-sites have been found as 110 m and 38 m, respectively [65]. Thus, the average wind speeds for Jal-Alayah and Wafra cell-sites have been adjusted as per (3), yielding 6.20 m/s and 5.97 m/s, respectively. Figure 6 illustrates the monthly average clearness index, GHI, and wind speed at Jal-Alayah and Wafra cell-sites, while Table 1 summarizes the average annual temperature, clearness index, GHI and wind speed data at Jal-Alayah and Wafra cell-sites, which have been obtained from the POWER database [40]. It should be noted that the NASA POWER database encompasses solar, wind, and meteorological data collected, updated, and averaged over 40 years [66,67]. This serves to ensure that the results obtained in this work are statistically valid and realistically coincide with practical systems.

From Table 1, it can be seen that the Wafra cell-site enjoys slightly higher average clearness index and GHI than Jal-Alayah cell-site, and thus is expected to have higher potential when using PV panels. Contrarily, the Jal-Alayah cell-site has higher average wind speed (and wind potential) than the Wafra cell-site and thus is expected to have higher potential for WTs.

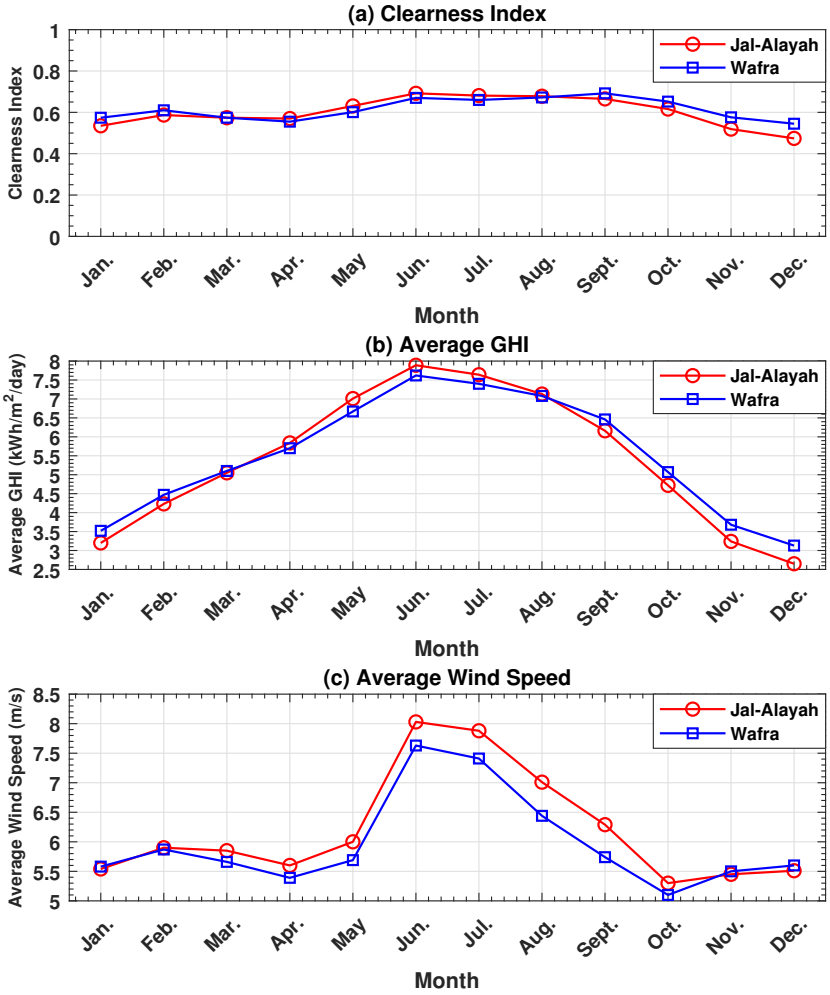

Figure 6. (**a**) Clearness Index, (**b**) Average GHI, and (**c**) Average Wind Speed of Jal-Alayah and Wafra cell-sites.

Table 1. Average annual characteristics of Jal-Alayah and Wafra cell-sites [40].

Cell-Site	Jal-Alayah	Wafra
Average Temperature (°C)	25.9	25.9
Clearness Index	0.60	0.62
Average GHI (kWh/m^2/day)	5.40	5.49
Average Wind Speed (m/s)	6.20	5.97
Height Above Sea Level (m)	110	38

4.3. Load Profiles

The BS load profiles of the Jal-Alayah and Wafra cell-sites have been obtained from mobile operator Zain, which is a leading mobile service provider in Kuwait and the Middle East [48]. The monthly DC load profiles for both cell-sites are depicted in Figure 7 for the period between June 2020 and May 2021. A summary of the load profiles is given in Table 2, where it can be seen that the Wafra cell-site consumes more power than the Jal-Alayah cell-site, which is due to the fact that Wafra encompasses farms and is surrounded by newly constructed residential buildings. The BSs at both cell-sites operate both 4G and 5G technologies, and they are configured as shown in Table 3.

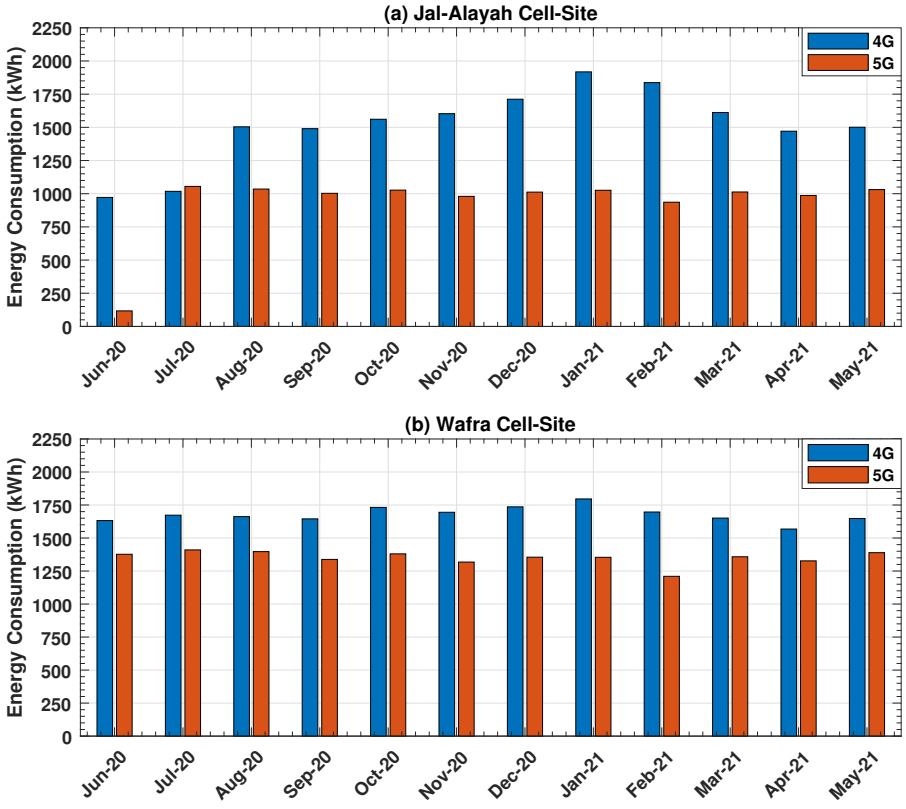

Figure 7. Base-station DC load profile at: (**a**) the Jal-Alayah cell-site and (**b**) the Wafra cell-site.

Table 2. Summary of load profiles at the Jal-Alayah and Wafra Cell-Sites.

Cell-Site	Jal-Alayah	Wafra
DC Load Annual Average (kWh/day)	80.4	99.4
Average DC Load Peak Power (kW)	9.94	12.3
AC Load Annual Average (kWh/day)	110	
Average AC Load Peak Power (kW)	13.6	
Total Load Annual Average (kWh/day)	190.4	209.4
Total Load Average Peak Power (kW)	23.5	25.9

Table 3. Base-station configuration at Jal-Alayah and Wafra Cell-Sites.

Technology	4G	5G
Number of Sectors	3	3
Number of Antennas per Sector	1	1
Output Power per Sector (W)	20, 40	200
Bandwidth per Sector (MHz)	10, 15, 20	100

4.4. Technical and Economic Specifications

In the following subsections, the technical and economic specifications of the main system components are detailed. The HPWES specifications are listed in Table 4 (It should be noted that the annual real interest rate—according to the Central Bank of Kuwait (CBK)—is 1.5% [68]).

Table 4. Control parameters and project lifetime.

Parameter	Value
Project Life Cycle (years)	20
Discount Rate (%)	2.6
Inflation Rate (%)	1.1
Annual Interest Rate (%)	1.5

4.4.1. PV Panels

The technical specifications of the mono-crystalline silicon (Mono-Si) PV panels used in this work are summarized in Table 5, whereas their detailed electro-mechanical specifications can be found in [58,59].

The Mono-Si PV panels have been utilized for the two-cell-sites in Kuwait due to their suitability for warmer weathers than the poly-crystalline silicon (Poly-Si) panels, as they happen to have relatively lower temperature coefficients (TCs) [69,70]. Specifically, the TC relates the drop in the output power of the PV panel to the increase in its temperature. On the other hand, the price in USD/kW per PV panel has been determined by reviewing numerous data sheets and surveying various vendors.

The annual output energy of a PV array (in kWh/yr) is calculated as [27]:

$$E_{pv} = \lambda_{pv} \times \xi_{\text{PSH}} \times f_{pv} \times 365 \text{ day/year}, \quad (4)$$

where λ_{pv} is the rated capacity of the PV array (in kW), while ξ_{PSH} is the peak solar irradiation-hour (in hours/day). Moreover, f_{pv} is the performance factor (i.e., solar cells efficiency) [27].

Table 5. PV panels and their specifications.

Panel	**CS6K-285M**	**SPR-P3-475-UPP**
Vendor	CanadianSolar	SunPower
Peak Power (W)	285	475
Dimensions (mm)	1650 × 992 × 40	2066 × 1160 × 35
Panel Area (m^2)	1.64	2.4
Temperature Range (°C)	−40 to 85	
Power Temperature Coefficient (%/°C)	−0.41	−0.34
Efficiency (%)	17.4	19.8
Initial Capital/Replacement Cost (USD/kW)	230	290
O&M Cost (USD/yr)	10	
Operational Lifetime (Years)	25	

4.4.2. Wind Turbines

In this paper, the selected horizontal-axis WTs are the Bergey Excel 10 kW and Eocycle 20 kW. Table 6 summarizes the technical specifications and costs of the wind turbine [60,61] (The O&M cost is set as 1% of the capital cost of the turbine [71]).

Table 6. Wind turbine technical data and cost.

Wind Turbine	**Bergey Excel**	**Eocycle**
Model	XL10	EO20
Rated Power (kW)	10	20
Life Expectancy (years)	20	20
Cut-In Wind Speed (m/s)	3.4	2.8
Cut-Out Wind Speed (m/s)	N/A	20
Rated Wind Speed (m/s)	15.6	7.5
Hub Height (m)	30	36
Rotor Diameter (m)	7	15.8
Number of Blades	3	3
Swept Area (m^2)	38.5	196.3
Initial Capital/Replacement Cost (USD)	13,400	34,000
O&M Cost (USD/year)	134	340

Wind speed distribution is the most important factor influencing the power available P_{av} in the wind [11], which is given by:

$$P_{av} = \frac{1}{2} A \rho V_w^3, \tag{5}$$

where $A = \pi R^2$ is the circular swept area of the blades, and R is the radius of the circle, which corresponds to the length of the one of blades. Moreover, $\rho = 1.225$ kg/m^3 is the air density at sea level, while V_w is the wind speed. The WT rated power is obtained at wind speed V_w, where $V_{rs} < V_w < V_{co}$, while V_{rs} and V_{co} are the rated and cut-out wind speeds, respectively [72]. In such a case, the produced power from the WT can be described by:

$$P_{WT} = P_{av} C_P, \tag{6}$$

where C_P is the Betz power coefficient. Ideally, the Betz coefficient reaches its maximum value of 59.3%, and in modern WTs, it can reach up to 50% [31].

4.4.3. Battery

A 11.7 kWh Lithium-ion battery is utilized, which is most suitable for standalone systems (despite its higher cost than a Lead-acid battery) [73], and the specifications of which are given in Table 7.

Table 7. Battery specifications.

Parameter	Value
Vendor	Sunverge
Battery Model	SIS-XWplus 6848
Nominal Voltage (V)	48
Nominal Capacity (kWh)	11.7
Nominal Charge (Ah)	244
Roundtrip Efficiency (%)	90
Maximum Charge Current (A)	110
Maximum Discharge Current (A)	125
Initial State-of-Charge (%)	100
Minimum State-of-Charge (%)	20
Maximum Depth-of-Discharge (%)	80
Initial Capital/Replacement Cost (USD)	1603
O&M Cost (USD/yr)	60

In general, the total capacity of the battery can be calculated as [64]:

$$C_B = \frac{E_L S_D}{V_B \times DoD_{\max} \times T_{cf} \times \eta_B}, \tag{7}$$

where E_L, S_D, V_B, $DoD_{\max}$, T_{cf}, and η_B are the load in Wh, storage days, battery voltage, maximum DoD, temperature correction factor, and battery efficiency, respectively [64]. On the other hand, the number of days of autonomy is determined using:

$$A_B = \frac{N_{bat} \times B_v \times B_Q \times B_{DoD} \times (24\,\mathrm{h/d})}{L_{BS}}, \tag{8}$$

where N_{bat} is the number of batteries in the battery storage. Moreover, B_v is the nominal battery voltage, while B_Q is the nominal capacity of a single battery (in Ah). In addition, B_{DoD} is the maximum energy delivered from the battery, whereas L_{BS} is the average daily BS load (in kWh). On the other hand, the battery lifetime can be obtained as [53]:

$$LT_B = \min\left(\frac{N_{bat} \times Q_{LT}}{Q_{Th}}, B_{bf}\right), \tag{9}$$

where Q_{LT} and Q_{Th} are the lifespan throughput of a battery (in kWh) and the annual battery throughput (in kWh), respectively. Moreover, B_{bf} is the battery float life (in years). The total number of batteries is $N_{batt}^{series} \times N_{batt}^{parallel}$, where the number of batteries connected in series is calculated as:

$$N_{batt}^{series} = \frac{V_{bb}}{B_v}, \tag{10}$$

in which V_{bb} is the DC bus bar voltage. The battery state-of-charge (SOC) is dependent on the hybrid energy sources, load demand, the efficiency of converter, battery bank, and the hourly self-discharge rate [64]. The SOC takes a value between C_B (as the maximum value), and $(1 - DoD_{\max}) \times C_B$ (as the minimum value). If the battery is depleted (i.e., reaches the maximum DoD), the DG can be utilized as a backup system [14].

4.4.4. Converter

A generic converter is utilized, with a lifetime of 15 years and efficiency of 95%. The converter specifications are given in Table 8.

Table 8. Converter Specifications.

Parameter	Value
Operational Lifetime (Years)	15
Efficiency (%)	95
Rectifier Relative Capacity (%)	100
Initial Capital/Replacement Cost (USD/kW)	310
O&M Cost (USD/Year)	10

4.4.5. Diesel Generator

As for the DG, the technical and economic specifications are shown in Table 9. In practice, and assuming regular maintenance, DGs can operate from 12,000 up to 20,000 h before needing major engine overhauls [74]. Lastly, it should be noted that the price of Diesel in Kuwait is 0.38 USD/L [75].

Table 9. Diesel generator specifications.

Parameter	Value
Fuel	Diesel
Operational Lifetime (Hours)	15,000
Fuel price (USD/L)	0.38
Initial Capital/Replacement Cost (USD/kW)	216
O&M Cost (USD/Operation Hour)	0.01

In general, the energy generated by a DG (in kWh) can be determined as:

$$E_{DG} = \tau \times P_{DG} \times \eta_{DG}, \tag{11}$$

where τ is the operation duration (in hours), P_{DG} is the DG rated output power, and η_{DG} is the efficiency of the DG. Moreover, the DG fuel consumption (in Liters) is calculated as:

$$F_c = F_{sfc} \times E_{DG}, \tag{12}$$

where F_{sfc} is the specific fuel consumption (in L/kWh).

4.4.6. Control Unit

Typically, two dispatch strategies can be used [76]: (a) cycle charging (CC), and (b) load following (LF). The CC strategy utilizes the DG to supply energy to the load and also uses excess energy to charge the BB. Contrarily, the LF strategy utilizes the DG to produce enough power to meet the BS load but does not charge the BB, as this is achieved via the PV panels and WTs.

4.5. HOMER Cost Model

HOMER calculates the cost of each system configuration, and ranks them in descending order based on NPC (and COE). The NPC of a system is based on the system life cycle cost C_{LCC}, including the initial capital cost C_{IC}, replacement cost C_{Rep}, and operation and maintenance (O&M) cost $C_{O\&M}$. Specifically, the C_{LLC} is mathematically expressed as:

$$C_{LCC} = C_{IC} + C_{Rep} + C_{O\&M}. \tag{13}$$

On the other hand, the NPC (USD) can be defined as:

$$NPC = \frac{C_{TAC}}{CRF}, \tag{14}$$

where C_{TAC} is the total production annualized cost (USD) (i.e., the annualized value of the total NPC), whereas CRF is the capital recovery factor (CRF). The CRF (USD) converts the NPC into a flow of equal annual interest payment over a specified period and is computed as [27]:

$$CRF = \frac{i(1+i)^n}{(1+i)^n - 1}, \tag{15}$$

where i is the real annual interest rate, and n is the project lifetime in years. The present value of cash flow occurs in any year of the project life-cycle and is calculated using discount factor ratio f_d as [27]:

$$f_d = \frac{1}{(1+i)^n}. \tag{16}$$

Lastly, the salvage cost is also estimated in HOMER, which refers to the residual value of the system components at the end of the project life time. Specifically, the salvage value S_v is determined as:

$$S_v = C_{C,Rep} \times \frac{C_{C,RTL}}{C_{C,LT}}, \tag{17}$$

where $C_{C,Rep}$, $C_{C,RLT}$, and $C_{C,LT}$ are the replacement cost, remaining lifetime, and lifetime of the component, respectively.

4.6. HOMER Performance Criteria

4.6.1. Cost of Energy

In HOMER, the COE (USD/kWh) is calculated as the ratio of the annual production cost to the total electric load supplied as follows:

$$COE = \frac{C_{TAC}}{AT_{dc} + AT_{ac}}, \tag{18}$$

where AT_{dc} (AT_{ac}) is the annualized total DC (AC) load served by the system.

4.6.2. Renewable Energy Fraction

The renewable energy fraction (REF) is determined as the ratio of the energy supplied by the renewable energy sources to the total energy produced by the system. Intuitively, the higher the REF is, the lower the CO_2 emissions are. The REF (%) can be calculated as:

$$REF = 1 - \frac{\sum E_{\mathrm{DG}}}{\sum E_{\mathrm{renewables}}}, \tag{19}$$

where E_{DG} is the energy supplied by the DG, while $E_{\mathrm{renewables}}$ is the energy supplied by the RESs (i.e., PV and/or WT).

4.6.3. CO_2 Emissions

HOMER calculates the CO_2 emissions using the emission factor (g/kWh) for CO_2, which is obtained for the amount of fuel consumed by the DG. Specifically, the DG emits 3.67 g of CO_2 for every g of carbon in the consumed diesel. Therefore, HOMER multiplies the total energy produced by the DG (in kWh) by the emission factor [77,78].

5. Simulation Results

This section evaluates the proposed HPWES design in the HOMER software package (version 3.13.8) with the aim of minimizing the NPC by determining the optimal system sizing—based on realistic economic factors and practical components—to meet the load demand of BSs at the two rural cell-sites. In the following subsections, the simulation results of the various system configurations in the Jal-Alayah and Wafra cell-sites are presented in terms of the system components, COE, NPC, REF, fuel consumption, and CO_2 emissions. In the simulations, a minimum of two days (i.e., 48 h) of autonomy is assumed (Conventionally, the battery bank should supply energy to the BS for 2–3 days of autonomy before reaching the maximum DoD [79]). Moreover, it has been determined that the CC dispatch strategy is the optimal strategy from the NPC perspective in all system configurations. This is particularly important in the scenario whereby whenever the DG needs to be on to meet the net load (load minus renewable power), it is ramped to charge the battery to the maximum extent possible [80].

5.1. Jal-Alayah Cell-Site—Case 1: 285 W PV Panel—10 kW WT

The simulation results for Case 1 are displayed in Table 10. The optimal configuration (in terms of NPC) is PV-DG-BB, which consists of 195 PV panels, 41 batteries, a 26 kW DG, and a converter of 14.2 kW. In addition, the PV-DG-BB configuration has a 95.2% REF, 2731 kg/yr CO_2 emissions, a total fuel consumption of 1043 L/yr, an NPC of USD 119,377, and a COE of USD 0.0999. On the other hand, the second optimal configuration is the PV-WT-DG-BB, which has lower CO_2 emissions (of 690 kg/yr) and a higher REF of 98.8%. Although the PV-BB, PV-WT-BB, and WT-BB configurations have a 100% REF and zero CO_2 emissions, they incur higher NPCs in comparison to the PV-DG-BB configuration.

Table 10. Simulation Results for Jal-Alayah Cell Site—Case 1.

	Configuration	PV-DG-BB	PV-WT-DG-BB	PV-BB	PV-WT-BB	WT-DG-BB	WT-BB
Optimal System Sizing	PV Array Capacity (kW)	55.3	47.8	108	95.5	-	-
	Number of Panels	195	168	379	336	-	-
	Number of WTs	-	1	-	1	3	6
	DG Rated Power (kW)	26	26	-	-	26	-
	Battery (Units)	41	41	41	41	41	41
	Converter Rated Power (kW)	14.2	14.0	13.8	15.7	21.0	21.0
	Renewable Energy Fraction (%)	95.2	98.8	100	100	90.5	100
Cost Factors	COE (USD)	0.0999	0.101	0.107	0.114	0.128	0.150
	NPC (USD)	119,377	121,228	128,026	135,734	152,913	179,040
Fuel Consumption & CO_2 Emissions	Total Fuel Consumption (L/yr)	1043	264	0	0	2043	0
	CO_2 Emissions (kg/yr)	2731	690	0	0	5347	0

5.2. Jal-Alayah Cell-Site—Case 2: 475 W PV Panel—10 kW WT

The simulation results for Case 2 is shown in Table 11. It can be seen that the optimal system configuration is PV-WT-DG-BB, which includes 80 PV panels, a 10 kW WT, 41 batteries, a 12.8 kW converter, and a 26 kW DG. The NPC is at USD 119,556, and the COE is USD 0.100, while the amount of CO_2 emissions is 826 kg/yr.

Table 11. Simulation Results for Jal-Alayah Cell Site—Case 2.

Configuration		PV-WT-DG-BB	PV-DG-BB	PV-BB	PV-WT-BB	WT-DG-BB	WT-BB
Optimal System Sizing	PV Array Capacity (kW)	38	53.1	105	95.5	-	-
	Number of Panels	80	187	369	336	-	-
	Number of WTs	1	-	-	1	3	6
	DG Rated Power (kW)	26	26	-	-	26	-
	Battery (Units)	41	41	42	41	41	41
	Converter Rated Power (kW)	12.8	14.1	13.7	15.7	21.0	21.0
	Renewable Energy Fraction (%)	98.6	94.8	100	100	905	100
Cost Factors	COE (USD)	0.100	0.102	0.112	0.118	0.128	0.150
	NPC (USD)	119,556	122,068	133,411	140,609	152,913	179,040
Fuel Consumption & CO_2 Emissions	Total Fuel Consumption (L/yr)	315	1133	0	0	2043	0
	CO_2 Emissions (kg/yr)	826	3611	0	0	6630	0

5.3. Jal-Alayah Cell-Site—Case 3: 285 W PV Panel—20 kW WT

For Case 3, the optimization results are presented in Table 12. The optimal system configuration is WT-BB with an NPC of USD 118,619 and a COE of USD 0.0993. Particularly, the WT-BB configuration consists of a 20 kW WT, 41 battery units, and a 11.1 kW converter. In addition, the WT-BB yields 100% REF and is the optimal configuration based on CO_2 emissions, as would be expected. On other hand, the PV-DG-BB is the second best configuration with slightly higher NPC than its WT-BB counterpart configuration, and about 2731 kg/yr of CO_2 emissions.

Table 12. Simulation Results for Jal-Alayah Cell Site—Case 3.

Configuration		WT-BB	PV-DG-BB	WT-DG-BB	PV-BB	PV-WT-DG-BB	PV-WT-BB
Optimal System Sizing	PV Array Capacity (kW)	-	55.3	-	108	47.8	95.5
	Number of Panels	-	195	-	379	168	336
	Number of WTs	1	-	1	-	1	1
	DG Rated Power (kW)	-	26	26	-	26	-
	Battery (Units)	41	41	41	41	41	43
	Converter Rated Power (kW)	11.1	14.2	11.6	13.8	14.0	10.5
	Renewable Energy Fraction (%)	100	95.2	99.4	100	100	100
Cost Factors	COE (USD)	0.0993	0.0999	0.102	0.107	0.115	0.129
	NPC (USD)	118,619	119,337	121,838	128,026	137,349	154,096
Fuel Consumption & CO_2 Emissions	Total Fuel Consumption (L/yr)	0	1043	163	0	0	0
	CO_2 Emissions (kg/yr)	0	2731	428	0	0	0

5.4. Jal-Alayah Cell-Site—Case 4: 475 W PV Panel—20 kW WT

The NPCs of the different configuration for Case 4 are given in Table 13. The WT-BB configuration is the optimal and is identical to Case 3. In addition, the WT-BB configuration has a 100% REF, and zero CO_2 emissions. By comparing Cases 3 and 4, it is clear that using the 20 kW WT eliminates the need for PV panels (i.e., neither the 285 W PV panel nor the 475 PV panel are needed).

Table 13. Simulation Results for Jal-Alayah Cell Site—Case 4.

Configuration		WT-BB	WT-DG-BB	PV-DG-BB	PV-BB	PV-WT-DG-BB	PV-WT-BB
Optimal System Sizing	PV Array Capacity (kW)	-	-	53.1	105	47.7	95.5
	Number of Panels	-	-	112	222	101	202
	Number of WTs	1	1	-	-	1	1
	DG Rated Power (kW)	-	26	26	-	26	-
	Battery (Units)	41	41	41	42	41	43
	Converter Rated Power (kW)	11.1	11.6	14.1	13.7	12.2	10.5
	Renewable Energy Fraction (%)	100	99.4	94.8	100	100	100
Cost Factors	COE (USD)	0.0993	0.102	0.102	0.112	0.116	0.133
	NPC (USD)	118,619	121,838	122,068	133,411	138,747	158,972
Fuel Consumption & CO_2 Emissions	Total Fuel Consumption (L/yr)	0	163	1133	0	5.97	0
	CO_2 Emissions (kg/yr)	0	428	2965	0	15.6	0

5.5. Jal-Alayah Cell-Site—DG-BB and DG-WBB Configurations

Table 14 summarizes the optimal sizing, cost factors, fuel consumption, and CO_2 emissions of the DG-BB and DG-WBB configurations. Clearly, the DG-WBB configurations incurs higher NPC than its DG-BB configurations, which is due to the absence of the BB, which implies that the DG operates continuously to supply the BS load demand, with no excess energy stored in the BB. This translates to higher fuel consumption, and CO_2 emissions. In comparison to Cases 1–4, it is clear that the conventional DG-BB and DG-WBB configurations are significantly worse from economic and environmental aspects.

Table 14. Simulation Results for Jal-Alayah—DG-BB and DG-WBB Configurations.

Configuration		DG-BB	DG-WBB
Optimal System Sizing	DG Rated Power (kW)	26	26
	Battery (Units)	41	-
	Converter Rated Power (kW)	20.7	8.42
Cost Factors	COE (USD)	0.238	0.265
	NPC (USD)	283,936	316,741
Fuel Consumption & CO_2 Emissions	Total Fuel Consumption (L/yr)	23,244	31,805
	CO_2 Emissions (kg/yr)	60,843	83,254

5.6. Wafra Cell-Site—Case 1: 285 W PV Panel—10 kW WT

The optimization results for Case 1 can be seen in Table 15. The PV-BB configuration yields the lowest NPC and COE, which are equal to USD 125,878 and USD 0.0958, respectively, and with zero CO_2 emissions. Particularly, this configuration consists of 294 PV panels, 45 batteries, and a 12.9 kW converter.

Table 15. Simulation Results for Wafra Cell Site—Case 1.

Configuration		PV-BB	PV-DG-BB	PV-WT-DG-BB	PV-WT-BB	WT-DG-BB	WT-BB
Optimal System Sizing	PV Array Capacity (kW)	83.6	60.3	52.5	78.1	-	-
	Number of Panels	294	212	185	275	-	-
	Number of WTs	-	-	1	1	4	9
	DG Rated Power (kW)	-	28	28	-	28	-
	Battery (Units)	45	45	45	45	45	45
	Converter Rated Power (kW)	12.9	15.0	12.3	13.1	22.0	12.4
	Renewable Energy Fraction (%)	100	97.0	99.5	100	94.5	100
Cost Factors	COE (USD)	0.0958	0.0962	0.0977	0.103	0.129	0.173
	NPC (USD)	125,878	126,457	128,399	135,168	170,064	227,181
Fuel Consumption	Total Fuel Consumption (L/yr)	0	735	141	0	1314	0
& CO_2 Emissions	CO_2 Emissions (kg/yr)	0	1923	368	0	3440	0

5.7. Wafra Cell-Site—Case 2: 475 W PV Panel—10 kW WT

In Table 16, the simulation results for each configuration for Case 2 are highlighted. Clearly, the optimal configuration is PV-DG-BB, while the second optimal configuration is PV-BB, which incurs slightly higher NPC, but with zero CO_2 emissions. From an environmental perspective, the PV-BB configuration could be used.

Table 16. Simulation Results for Wafra Cell Site—Case 2.

Configuration		PV-DG-BB	PV-BB	PV-WT-DG-BB	PV-WT-BB	WT-DG-BB	WT-BB
Optimal System Sizing	PV Array Capacity (kW)	57.4	82.6	52.5	78.1	-	-
	Number of Panels	121	174	111	165	-	-
	Number of WTs	0	0	1	1	4	9
	DG Rated Power (kW)	28	-	28	-	28	-
	Battery (Units)	45	45	45	45	45	45
	Converter Rated Power (kW)	14.2	13.3	12.3	13.1	22.0	12.4
	Renewable Energy Fraction (%)	96.4	100	99.5	100	94.5	100
Cost Factors	COE (USD)	0.0983	0.0989	0.0997	0.106	0.129	0.173
	NPC (USD)	129,153	129,965	131,030	139,152	170,064	227,181
Fuel Consumption	Total Fuel Consumption (L/yr)	878	0	135	0	1314	0
& CO_2 Emissions	CO_2 Emissions (kg/yr)	2299	0	353	0	3440	0

5.8. Wafra Cell-Site—Case 3: 285 W PV Panel—20 kW WT

The simulation results for Case 3 are given in Table 17. The optimal configuration is PV-BB, which consists of 294 PV solar panels, 45 batteries, a 28 kW DG, and a converter of 12.9 kW. In addition, the PV-BB configuration has a 100% REF, zero CO_2 emissions, an NPC of USD 125,878, and a COE of USD 0.0958. Moreover, the second optimal configuration is the PV-DG-BB, which has CO_2 emissions of 1923 kg/yr and an REF of 97%.

Table 17. Simulation Results for Wafra Cell Site—Case 3.

Configuration		PV-BB	PV-DG-BB	WT-DG-BB	PV-WT-DG-BB	PV-WT-BB	WT-BB
Optimal System Sizing	PV Array Capacity (kW)	83.6	60.3	-	52.5	78.1	-
	Number of Panels	294	212	-	185	275	-
	Number of WTs	0	0	1	1	1	2
	DG Rated Power (kW)	0	28	28	28	0	0
	Battery (Units)	45	45	45	45	45	45
	Converter Rated Power (kW)	12.9	15.0	12.0	12.3	13.1	9.03
	Renewable Energy Fraction (%)	100	97.0	97.4	100	100	100
Cost Factors	COE (USD)	0.0958	0.0962	0.103	0.110	0.117	0.124
	NPC (USD)	125,878	126,457	135,046	145,060	153,201	162,547
Fuel Consumption	Total Fuel Consumption (L/yr)	0	735	747	6.43	0	0
& CO_2 Emissions	CO_2 Emissions (kg/yr)	0	1923	1957	16.8	0	0

5.9. Wafra Cell-Site—Case 4: 475 W PV Panel—20 kW WT

Table 18 summarizes the simulation results for Case 4. The PV-DG-BB configuration has the lowest NPC and COE, which are equal to USD 129,153 and USD 0.0989, respectively. In addition, the REF is 96.4% with 2299 kg/yr of CO_2 emissions. On the other hand, the PV-BB configuration has the second best NPC and COE, with 100% REF and zero CO_2 emissions. Notably, the PV-BB configuration is more preferred from an environmental perspective, with a negligible increase in the NPC.

Table 18. Simulation Results for Wafra Cell Site—Case 4.

Configuration		PV-DG-BB	PV-BB	WT-DG-BB	PV-WT-DG-BB	PV-WT-BB	WT-BB
Optimal System Sizing	PV Array Capacity (kW)	57.4	82.6	-	52.5	78.1	-
	Number of Panels	121	174	-	111	165	-
	Number of WTs	-	-	1	1	1	2
	DG Rated Power (kW)	28	-	28	28	-	-
	Battery (Units)	45	45	45	45	45	45
	Converter Rated Power (kW)	14.2	13.3	12.0	12.3	13.1	9.03
	Renewable Energy Fraction (%)	96.4	100	97.4	100	100	100
Cost Factors	COE (USD)	0.0983	0.0989	0.103	0.112	0.120	0.124
	NPC (USD)	129,153	129.965	135,046	147,738	157,187	162,547
Fuel Consumption	Total Fuel Consumption (L/yr)	878	0	747	6.43	0	0
& CO_2 Emissions	CO_2 Emissions (kg/yr)	2299	0	1957	16.8	0	0

5.10. Wafra Cell-Site—DG-BB and DG-WBB Configurations

Table 19 gives the technical, economic, and environmental results of the DG-BB and DG-WBB configurations. Evidently, the DG-WBB configuration incurs a higher NPC and COE than the DG-BB configuration, with higher fuel consumption and CO_2 emissions. More importantly, the DG-BB and DG-WBB configurations are inferior to the optimal configurations of Cases 1 to 4.

Table 19. Simulation Results for Wafra—DG-BB and DG-WBB Configurations.

Configuration		DG-BB	DG-WBB
Optimal System Sizing	DG Rated Power (kW)	28	28
	Battery (Units)	45	-
	Converter Rated Power (kW)	22.6	10.5
Cost Factors	COE (USD)	0.236	0.262
	NPC (USD)	310,414	343,801
Fuel Consumption & CO_2 Emissions	Total Fuel Consumption (L/yr)	25,509	34,624
	CO_2 Emissions (kg/yr)	66,773	90,633

5.11. Summary of Findings

5.11.1. Jal-Alayah Cell-Site

The optimal system configurations of each case for Jal-Alayah cell-site are summarized in Table 20. The WT-BB configuration in Cases 3 and 4 is the most cost-effective, as it yields the minimum NPC. Clearly, utilizing the 20 kW WT is optimal, irrespective of the PV panel used, which implies that a single 20 kW WT eliminates the need for PV panels and the DG to meet the load demand at the Jal-Alayah cell-site and with minimal cost. More importantly, the WT-BB configuration is not only the optimal system in terms of NPC but also in terms of CO_2 emissions, REF, and required land area (of 258 m^2) (For one WT, the land area is small. For safety purposes, 5 m is added to rotor diameter on both sides, and 5 m is added to the front and back of the WT. In practice, and in the case of more than one WT, the WTs spacing is calculated as discussed in [81]. However, a single WT suffices to meet the BS load demand in this work). On the other hand, the PV-DG-BB is the second optimal configuration in the Case 1, with NPC of USD 119,377 and land area of 735.6 m^2. The PV-WT-DG-BB configuration in Case 2 has the third best NPC and second best in terms of land area (of 611.6 m^2) (Area = (PV panel area $\times$ number of PV panels $\times \xi$) + (WT rotor diameter + 10 m) $\times$ 10 m, where $\xi = 2.3$ is the shading factor [82,83]). Clearly, the PV-WT-DG-BB configuration incurs a marginal increase in the NPC in comparison to the PV-DG-BB configuration, but yields lower CO_2 emissions and higher REF.

Table 20. Comparison of optimal configurations for Jal-Alayah cell-site.

Case	Optimal Configuration	NPC (USD)	No. PV Panels	No. Wind Turbines	Fuel Consumption (L/yr)	CO_2 Emissions (kg/yr)	Renewable Energy Fraction (%)	Land Area (m^2)
1	PV-DG-BB	119,377	195	0	1043	2731	95.2	735.6
2	PV-WT-DG-BB	119,556	80	1	315	826	98.6	611.6
3	WT-BB	118,619	0	1	0	0	100	258
4	WT-BB	118,619	0	1	0	0	100	258

Figure 8 illustrates the monthly energy production in Jal-Alayah cell-site for the optimal configurations given in Table 20. Particularly, Figure 8a depicts the energy production for the PV-DG-BB configuration of Case 1. It can be seen that the DG is operated to meet the BS load demand in the Winter months of November 2020 to March 2021, which is attributed to the low average GHI in those months. Clearly, the PV energy production is significantly higher than that of the DG, which yields an REF of 95.2%. In Figure 8b, the energy production of the the PV-WT-DG-BB configuration of Case 2 is shown. Evidently, the WT and PV produce most of the required energy to operate the BS (with REF of 98.6%), while the DG is only used during the months of November 2020 to December 2020. Lastly, Figure 8c demonstrates the energy production of the WT-BB configuration for Cases 3 and 4. It is clear that the WT solely supplies the BS, yielding 100% REF.

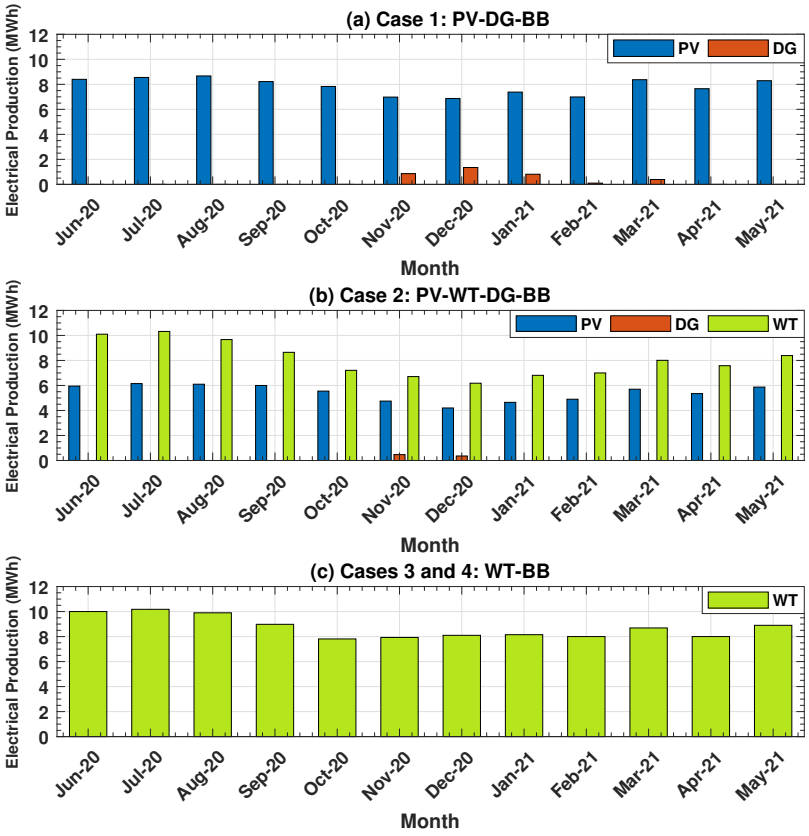

Figure 8. Monthly energy production at Jal-Alayah cell-site for: (**a**) Case 1: PV-DG-BB, (**b**) Case 2: PV-WT-DG-BB, and (**c**) Cases 3 and 4: WT-BB.

In Figure 9 summarizes the NPC savings of the optimal configurations presented in Table 20 to the conventional DG-BB and DG-WBB configurations presented in Table 14. In particular, one can see that the optimal configurations yield about 58% (62%) of NPC saving in comparison to the DG-BB (DG-WBB) configuration.

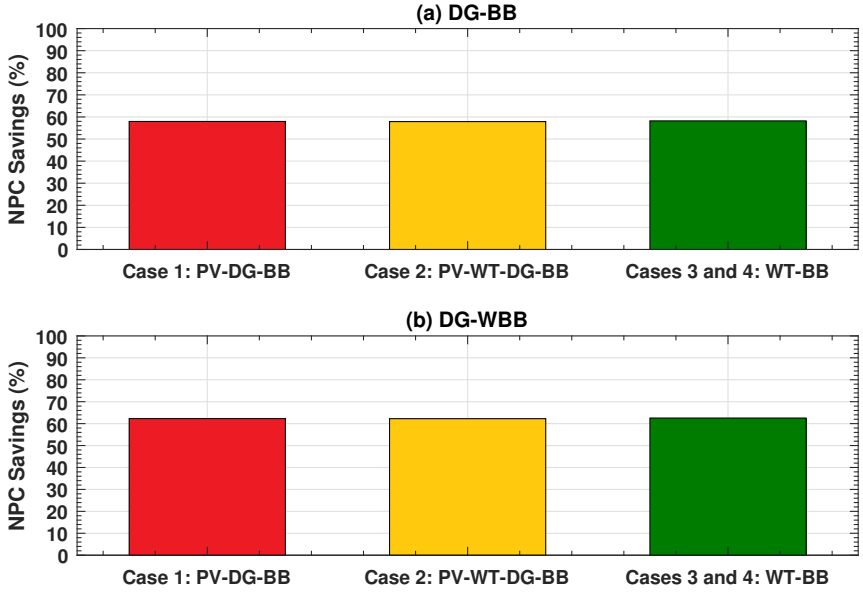

Figure 9. NPC savings of Jal-Alayah cell-site with respect to the: (**a**) DG-BB and (**b**) DG-WBB configurations.

5.11.2. Wafra Cell-Site

Referring to Table 21, the PV-BB configuration in Cases 1 and 3 has the lowest NPC, with 100% REF and zero CO_2 emissions. This implies that using a WT is not economic in this cell-site, and the 285 W PV panels suffice to meet the BS load demand. On the other hand, the PV-DG-BB configuration in the Cases 2 and 4 is the second best configuration in terms of the NPC and with the use of the WT being not economic. Moreover, in terms of the required land area, the PV-DG-BB configuration with the 475 W PV panel is the best, but at the expense of a minor increase in the NPC and an REF of 96.4%. Generally speaking, rural areas are not constrained by land space, and thus, the PV-BB would be more desirable, as it achieves zero CO_2 emissions. However, if this is not the case, then the PV-DG-BB configuration with the 475 W PV panels can be used.

Table 21. Comparison of optimal configurations for the Wafra cell-site.

Case	Optimal Configuration	NPC (USD)	No. PV Panels	No. Wind Turbines	Fuel Consumption (L/yr)	CO_2 Emissions (kg/yr)	Renewable Energy Fraction (%)	Land Area (m^2)
1	PV-BB	125,878	294	0	0	0	100	1109
2	PV-DG-BB	129,153	121	0	878	2299	96.4	668
3	PV-BB	125,878	294	0	0	0	100	1109
4	PV-DG-BB	129,153	121	0	878	2299	96.4	668

Figure 10a demonstrates the monthly energy production of the optimal configuration PV-BB of Cases 1 and 3, which solely depend on the PV panels (i.e., 100% REF). Notably, the lowest energy production occurs in November 2020 to February 2021. On the other hand, Figure 10b depicts the energy production of the optimal configuration PV-DG-BB for Cases 2 and 4. It is clear that the DG only operates to serve the BS load during the months of November 2020 to March 2021, while the PV panels yield 96.4% REF.

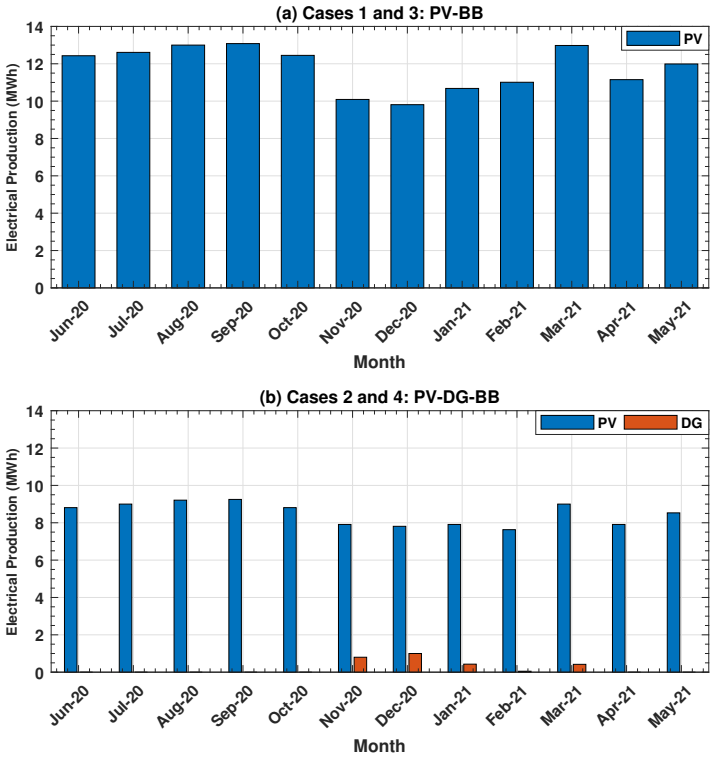

Figure 10. Monthly energy production at Wafra cell-site for: (**a**) Cases 1 and 3: PV-BB, and (**b**) Cases 2 and 4: PV-DG-BB.

The NPC savings of the optimal configurations given in Table 21 in comparison to the DG-BB and DG-WBB configurations presented in Table 19 are shown in Figure 11. Similar observations to those given in Figure 9 can be made. In general, the NPC savings with respect to the DG-WBB configuration are greater than those of DG-BB.

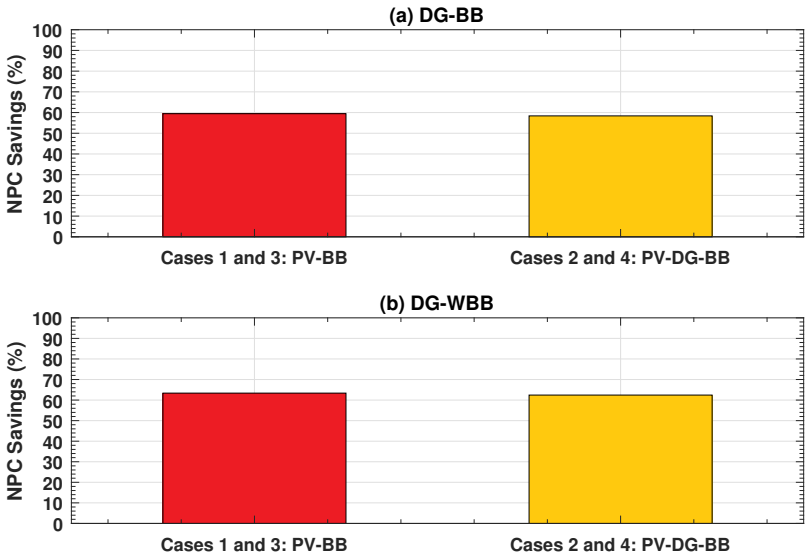

Figure 11. NPC savings of Wafra cell-site with respect to the (**a**) DG-BB and (**b**) DG-WBB configurations.

5.11.3. Jal-Alayah Cell-Site vs. Wafra Cell-Site

By comparing Tables 20 and 21, it is evident that utilizing a WT is only beneficial to the Jal-Alayah cell-site (in terms of the NPC). This is due to the fact that Jal-Alayah has higher annual average wind speed than the Wafra cell-site (see Table 1), which implies higher wind potential (This is in addition to the greater height above sea level. Recall that the Jal-Alayah and Wafra cell-sites are 110 m and 38 m above sea level, respectively). On the other hand, the Wafra cell-site enjoys slightly higher clearness index and annual average GHI than Jal-Alayah (see Table 1), which makes the use of PV panels more rewarding in terms of electricity production. This can be seen from Figure 12, which presents the annualized capacity factor of utilizing the PV panels and WTs at both cell-sites (The capacity factor defines the actual electrical energy output to the maximum possible electrical energy output over a given period of time [84]). In addition, one can see that the 20 kW WT yields significantly higher capacity factor than the 10 kW WT, which explains its dominance for Jal-Alayah (see Table 20).

In general, the WT-BB is the optimal configuration (in terms of the NPC) at the Jal-Alayah cell-site, when the 20 kW WT is utilized. As for the Wafra cell-site, utilizing the 285 W PV panels is the most cost-effective RES, with the PV-BB configuration being the most optimal in terms of NPC and REF. In turn, the WT-BB and PV-BB configurations can respectively be utilized in the Jal-Alayah and Wafra cell-sites to achieve zero CO_2 emissions while yielding the lowest NPC. Notably, in both cell-sites, the DG-BB and DG-WBB were the worst configurations in terms of NPC and CO_2 emissions (see Tables 14 and 19), which signifies the importance of utilizing RESs to satisfy the load demands of BSs in the rural areas of Kuwait. Lastly, in the obtained optimal configuration at each cell-site, the number of days of autonomy is 2.0167 (i.e., 48.4 h), which is in agreement with [79].

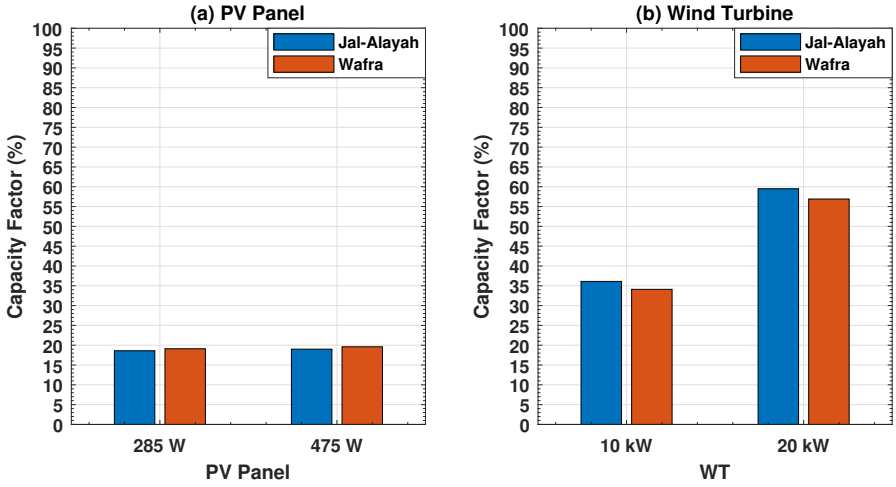

Figure 12. Capacity factor at Jal-Alayah and Wafra cell-sites for using (**a**) a PV Panel and (**b**) a Wind Turbine.

6. Conclusions

In this paper, the potentials of utilizing hybrid renewable-energy-powered BSs in Kuwait's rural areas have been examined to minimize both the NPC and CO_2 emissions. Initially, the HPWES system design, configurations, and techno-economic specifications have been defined. In particular, various system configurations have been considered, while utilizing different PV panels and WTs. Then, two cell-sites—namely, (1) Jal-Alayah and (2) Wafra—have been carefully selected based on their solar and wind potentials. The simulation results have revealed that utilizing a WT with a battery bank is the most economical configuration at the Jal-Alayah cell-site. On the other hand, the use of solar PV panels with a battery bank is the most cost-effective at the Wafra cell-site. For both of the aforementioned system configurations, 100% renewable energy and zero CO_2 emissions have been achieved. Additionally, different tradeoffs in terms of NPC, CO_2, and required land area have been revealed in both cell-sites. Finally, it can be confirmed that utilizing RESs in two rural areas in Kuwait can be extremely effective in replacing the conventional DG-powered BSs while minimizing the NPC and completely eliminating CO_2 emissions.

Author Contributions: M.W.B.: conceptualization; data curation; funding acquisition; project administration; investigation; supervision; writing—original draft; writing—review and editing. M.F.A.: investigation; software; validation; writing—original draft; writing—review and editing. R.M.K.: formal analysis; investigation; supervision; validation; writing—review and editing. S.S.A.: formal analysis; visualization; validation; writing—review and editing. All authors have read and agreed to the published version of the manuscript.

Funding: This work was partially supported by the Kuwait Foundation for the Advancement of Sciences (KFAS) under project code PN17-15EE-02.

Institutional Review Board Statement: Not applicable.

Informed Consent Statement: Not applicable.

Data Availability Statement: Data sharing is not applicable to this article.

Acknowledgments: Sincere gratitude and appreciation are extended to Nawaf Al-Gharabally, Chief Technology Officer (CTO), Zain, and for Omar Al-Saleh, Radio Networks Optimization Division, Zain, for providing the BSs' technical specifications and load profiles.

Conflicts of Interest: The authors declare no conflict of interest. The funders had no role in the design of the study; in the collection, analyses, or interpretation of data; in the writing of the manuscript, or in the decision to publish the results.

References

1. Dangi, R.; Lalwani, P.; Choudhary, G.; You, I.; Pau, G. Study and Investigation on 5G Technology: A Systematic Review. *Sensors* **2021**, *22*, 26. [CrossRef] [PubMed]
2. Freitag, C.; Berners-Lee, M.; Widdicks, K.; Knowles, B.; Blair, G.S.; Friday, A. The real climate and transformative impact of ICT: A critique of estimates, trends, and regulations. *Patterns* **2021**, *2*, 100340. [CrossRef] [PubMed]
3. Alsharif, M.H.; Nordin, R.; Ismail, M. Survey of Green Radio Communication Networks: Techniques and Recent Advances. *J. Comput. Netw. Commun.* **2013**, *2013*, 453893. [CrossRef]
4. Alsharif, M.H.; Nordin, R.; Ismail, M. Classification, Recent Advances and Research Challenges in Energy Efficient Cellular Networks. *Wirel. Pers. Commun.* **2014**, *77*, 1249–1269. [CrossRef]
5. Alsharif, M.H. Techno-Economic Evaluation of a Stand-Alone Power System Based on Solar Power/Batteries for Global System for Mobile Communications Base Stations. *Energies* **2017**, *10*, 392. [CrossRef]
6. Gandotra, P.; Jha, R.K.; Jain, S. Green Communication in Next Generation Cellular Networks: A Survey. *IEEE Access* **2017**, *5*, 11727–11758. [CrossRef]
7. Rathore, R.S.; Sangwan, S.; Kaiwartya, O.; Aggarwal, G. Green Communication for Next-Generation Wireless Systems: Optimization Strategies, Challenges, Solutions, and Future Aspects. *Wirel. Commun. Mob. Comput.* **2021**, *2021*, 5528584. [CrossRef]
8. Hu, J.L.; Chen, Y.C.; Yang, Y.P. The Development and Issues of Energy-ICT: A Review of Literature with Economic and Managerial Viewpoints. *Energies* **2022**, *15*, 594. [CrossRef]
9. Hossain, M.S.; Islam, K.Z.; Jahid, A.; Rahman, K.M.; Ahmed, S.; Alsharif, M.H. Renewable Energy-Aware Sustainable Cellular Networks with Load Balancing and Energy-Sharing Technique. *Sustainability* **2020**, *12*, 9340. [CrossRef]
10. Suraweera, H.A.; Yang, J.; Zappone, A.; Thompson, J. *Green Communications for Energy-Efficient Wireless Systems and Networks*; IET Digital Library: London, UK, 2020. [CrossRef]
11. Jadallah, A.A.; Mahmood, D.Y.; Er, Z.; Abdulqaedr, Z. Hybridization of Solar/Wind Energy System for Power Generation in Rural Areas. *Acta Phys. Pol. A* **2016**, *130*, 434–437. [CrossRef]
12. Jung, K.J.; Park, K.H.; Ko, Y.C.; Alouini, M.S. Renewable Energy-Enabled Cellular Networks. *SSRN* **2021**, 1–33. Available online: https://papers.ssrn.com/sol3/papers.cfm?abstract_id=3967953 (accessed on 1 February 2022). [CrossRef]
13. Chamola, V.; Sikdar, B. Solar Powered Cellular Base Stations: Current Scenario, Issues and Proposed Solutions. *IEEE Commun. Mag.* **2016**, *54*, 108–114. [CrossRef]
14. Alsharif, M.H. Comparative Analysis of Solar Powered Base Stations for Green Mobile Networks. *Energies* **2017**, *10*, 1208. [CrossRef]
15. Acharya, B.; Dutta, A. Solar and Wind Hybrid Power for an Extremely Remote Mobile Base Station. *Guelph Eng. J.* **2013**, *5*, 96–112.
16. Aris, A.M.; Shabani, B. Sustainable Power Supply Solutions for Off-Grid Base Stations. *Energies* **2015**, *8*, 10904–10941. [CrossRef]
17. Yeshalem, M.T.; Khan, B. Design of an Off-Grid Hybrid PV/Wind Power System for Remote Mobile Base Station: A Case Study. *AIMS Energy* **2017**, *5*, 96–112. [CrossRef]
18. HOMER Pro. Net Present Cost. Available online: https://www.homerenergy.com/products/pro/docs/latest/net_present_cost.html (accessed on 1 February 2022).
19. HOMER Pro. Cost of Energy. Available online: https://www.homerenergy.com/products/pro/docs/latest/levelized_cost_of_energy.html (accessed on 1 February 2022).
20. Alsharif, M.H.; Kannadasan, R.; Jahid, A.; Albreem, M.A.; Nebhen, J.; Choi, B.J. Long-Term Techno-Economic Analysis of Sustainable and Zero Grid Cellular Base Station. *IEEE Access* **2021**, *9*, 54159–54172. [CrossRef]
21. Alsharif, M.H.; Kim, J. Optimal Solar Power System for Remote Telecommunication Base Station: A Case Study Based on the Characteristics of South Korea's Solar Radiation Exposure. *Sustainability* **2016**, *8*, 942. [CrossRef]
22. Jahid, A.; Hossain, M.S.; Monju, M.K.H.; Rahman, M.F.; Hossain, M.F. Techno-Economic and Energy Efficiency Analysis of Optimal Power Supply Solutions for Green Cellular Base Stations. *IEEE Access* **2020**, *8*, 43776–43795. [CrossRef]
23. Babatunde, O.M.; Denwigwe, I.H.; Babatunde, D.E.; Ayeni, A.O.; Adedoja, T.B.; Adedoja, O.S. Techno-Economic Assessment of Photovoltaic-Diesel Generator-Battery Energy System for Base Transceiver Stations Loads in Nigeria. *Cogent Eng.* **2019**, *6*, 1684805. [CrossRef]
24. Oviroh, P.O.; Jen, T.C. The Energy Cost Analysis of Hybrid Systems and Diesel Generators in Powered Selected Base Transceiver Station Locations in Nigeria. *Energies* **2018**, *11*, 687. [CrossRef]
25. Asif, R.M.; Khanzada, F. Cellular Base Station Powered by Hybrid Energy Options. *Int. J. Comput. Appl.* **2015**, *115*, 35–39. [CrossRef]
26. Alsharif, M.H.; Raju, K.; Jahid, A.; Albreem, M.A.; Uthansakul, P.; Nebhen, J.; Chandrasekaran, V. Optimal Cost-Aware Paradigm for Off-Grid Green Cellular Networks in Oman. *Comput. Mater. Contin.* **2021**, *68*, 2665–2680. [CrossRef]
27. Alsharif, M.H.; Nordin, R.; Ismail, M. Energy Optimization of Hybrid Off Grid System for Remote Telecommunication Base Station Deployment in Malaysia. *EURASIP J. Wirel. Commun. Netw.* **2015**, *2015*, 64. [CrossRef]
28. Wikipedia. State of Kuwait. Available online: https://en.wikipedia.org/wiki/Kuwait (accessed on 1 February 2022).
29. Bou-Rabee, M.A.; Suliman, S.A.; Choe, G.; Han, D.; Saeed, T.; Marafie, S. Characteristics of Solar Energy Radiation on Typical Summer and Winter Days in Kuwait. *Int. J. Automot. Mech. Eng.* **2015**, *12*, 2944–2953. [CrossRef]
30. Ministry of Electricity, Water and Renewable Energy, Kuwait. Electrical Energy. In *Statistical Year Book*; Ministry of Electricity: Kuwait City, Kuwait, 2021. Available online: https://www.mew.gov.kw/en/about/statistics/ (accessed on 1 February 2022).

31. Hajiah, A.; Sebzali, M. Optimal Sizing of Wind Power Systems in Three High Wind Potential Zones in Kuwait for Remote Housing Electrification. *Int. J. Renew. Energy Res.* **2013**, *3*, 167–171.
32. Al-Fadhil, K. MEW Future to Come. Minister of Electricity and Water. 2019. Available online: https://www.mew.gov.kw/en/NewsDetails?fromurl=home&&newsname=FutToCome (accessed on 1 February 2022).
33. Alsaad, M. The Unsustainability of Kuwait's Energy System—Examining Kuwait's Energy Problem. The London School of Economics and Political Science—Blog. Available online: https://blogs.lse.ac.uk/mec/2021/02/11/the-unsustainability-of-kuwaits-energy-system-examining-kuwaits-energy-problem/ (accessed on 1 February 2022).
34. Arab Times. Housing Crisis Worsens as Kuwaitis' Requests for Homes Continue to Rise. Available online: https://www.arabtimesonline.com/news/housing-crisis-worsens-as-kuwaitis-requests-for-homes-continue-to-rise/ (accessed on 1 February 2022).
35. Al-Enezi, F.Q.; Sykulski, J.K.; Ahmed, N.A. Visibility and Potential of Solar Energy on Horizontal Surface at Kuwait Area. *Energy Procedia* **2011**, *12*, 862–872. [CrossRef]
36. Sebzali, M.; Hajiah, A.; Ebrahim, S. Analysis of Wind Power Potential Characteristics and Feasibility in Kuwait for Possible Electricity Production. *Int. J. Renew. Energy Res.* **2013**, *3*, 812–818.
37. Alotaibi, O.; Hussain, S. A Geographical Spatial Analysis on the Benefits of Using Wind Energy in Kuwait. *Energy Power Eng.* **2018**, *12*, 645–650.
38. Hadi, M.A.; Abdel-Razek, R.H.; Chakroun, W.M. Economic Assessment of the Use of Solar Energy in Kuwait. *Glob. J. Bus. Res.* **2015**, *7*, 73–82.
39. HOMER Pro. Global Horizontal Irradiance (GHI). Available online: https://www.homerenergy.com/products/pro/docs/latest/global_horizontal_irradiance_ghi.html (accessed on 1 February 2022).
40. The POWER Project. Available online: https://power.larc.nasa.gov/data-access-viewer/ (accessed on 1 February 2022).
41. Al-Nassar, W.; Alhajraf, S.; Al-Enizi, A.; Al-Awadhi, L. Potential Wind Power Generation in the State of Kuwait. *Int. J. Renew. Energy Res.* **2005**, *30*, 2149–2161. [CrossRef]
42. Steensma, G.; Roman, R.; Marshall, C.; Bermejo, J.; Iyer, K.; AL-Hajraf, S.; AL-Qattan, A. Shagaya Renewable Energy Park Project. *AIP Conf. Proc.* **2019**, *2126*, 040003. [CrossRef]
43. Altaneeb, S. Development of Renewable Energy in Kuwait. In Proceedings of the SPE Kuwait Oil & Gas Show and Conference, Mishref, Kuwait, 13 October 2019. [CrossRef]
44. Oxford Business Group. New Solar and Wind Capacity Will Move Kuwait Closer to Its 2030 Renewable Energy Generation Goals. Available online: https://oxfordbusinessgroup.com/analysis/winds-change-new-solar-and-wind-capacity-will-move-country-closer-its-2030-renewable-generation (accessed on 1 February 2022).
45. Al-Husainan, H. An Analysis of Wind and Solar Energy Resources for the State of Kuwait. Ph.D. Thesis, University of Oklahoma, Norman, Oklahoma, 2012. Available online: https://hdl.handle.net/11244/319313 (accessed on 1 February 2022).
46. World Bank. Mobile Cellular Subscriptions (per 100 People)—Kuwait. Available online: https://data.worldbank.org/indicator/IT.CEL.SETS.P2?locations=KW (accessed on 1 February 2022).
47. The Global Economy. Kuwait: Mobile Phone Subscribers. Available online: https://www.theglobaleconomy.com/Kuwait/ (accessed on 1 February 2022).
48. ZAIN Group. Available online: https://www.zain.com/en/ (accessed on 1 February 2022).
49. Ooredoo Group. Available online: https://www.ooredoo.com.kw/portal/en/company_overview (accessed on 1 February 2022).
50. Kuwait Telecommunication Company—STC. Available online: https://www.stc.com.kw/ (accessed on 1 February 2022).
51. Kusakana, K.; Vermaak, H.J. Hybrid Renewable Power Systems for Mobile Telephony Base Stations in Developing Countries. *Renew. Energy* **2013**, *51*, 419–425. [CrossRef]
52. HOMER Energy. Available online: https://www.homerenergy.com/ (accessed on 1 February 2022).
53. Lambert, T.W.; Gilman, P.; Lilienthal, P. *Micropower System Modeling with* HOMER*: Integration of Alternative Sources of Energy*; Farret, F.A., Simões, M.G., Eds.; John Wiley & Sons: Hoboken, NJ, USA, 2005.
54. Lilienthal, P.D.; Lambert, T.W.; Gilman, P. Computer Modeling of Renewable Power Systems. *Encycl. Energy* **2004**, *1*, 633–647.
55. Baidas, M.W.; Hasaneya, R.W.; Kamel, R.M.; Alanzi, S.S. Solar-Powered Cellular Base Stations in Kuwait: A Case Study. *Energies* **2021**, *17*, 7494. [CrossRef]
56. Aeolos Wind Turbine. Available online: https://www.windturbinestar.com/hawt-vs-vawt.html (accessed on 1 February 2022).
57. Khillar, S. Difference between Horizontal and Vertical Axis Wind Turbine. 2019. Available online: http://www.differencebetween.net/technology/difference-between-horizontal-and-vertical-axis-wind-turbine/ (accessed on 1 February 2022).
58. Canadian Solar-CS6K-285M Datasheet. Available online: https://www.solaris-shop.com/content/CS6K-285M-T4%20Specs.pdf (accessed on 1 February 2022).
59. Sunpower-SPR-P3-475-UPP Datasheet. Available online: https://sunpower.maxeon.com/au/sites/default/files/2020-12/sp_mst_P3_UPP_35mm_ds_AU.pdf (accessed on 1 February 2022).
60. Bergey Wind Power XL10. Available online: http://www.bergey.com/products/grid-tied-turbines/excel-10/ (accessed on 1 February 2022).
61. Eocycle EO20. Available online: https://en.wind-turbine-models.com/turbines/1640-eocycle-eo20 (accessed on 1 February 2022).

62. HOMER Pro. Weibull Distribution. Available online: https://www.homerenergy.com/products/pro/docs/latest/weibull_distribution.html (accessed on 1 February 2022).
63. Gradshteyn, I.S.; Ryshik, I.M. *Table of Integrals, Series and Products*, 7th ed.; Academic Press: New York, NY, USA, 2007.
64. Kaabeche, A.; Belhaml, M.; Ibtiouen, R. Optimal Sizing Method for Stand-Alone Hybrid PV/Wind Power Generation System. *Revue des Energies Renouvelables* **2015**, *1*, 205–213.
65. Map Tools Elevation Finder. Available online: https://www.freemaptools.com/elevation-finder.htm (accessed on 1 February 2022).
66. NASA's Open Data Portal—Prediction of Worldwide Energy Resources (POWER). Available online: https://data.nasa.gov/Earth-Science/Prediction-Of-Worldwide-Energy-Resources-POWER-/wn3p-qsan/data?pane=manage (accessed on 13 March 2022).
67. National Aeronautics and Space Administration—NASA POWER Project Powers up with New Version. Available online: https://www.nasa.gov/press-release/langley/nasa-power-project-powers-up-with-new-version (accessed on 13 March 2022).
68. CBK Press Releases. Available online: https://www.cbk.gov.kw/en (accessed on 1 February 2022).
69. Khalis, M.; Masrour, R.; Khrypunov, G.; Kirichenko, M.; Kudiy, D.; Zazoui, M. Effect Temperature and Concentration Mono and Polycrystalline Silicon Solar Cells: Extraction Parameters. *J. Phys. Conf. Ser.* **2016**, *758*, 012001. [CrossRef]
70. Adeeb, J.; Farhan, A.; Al-Salaymeh, A. Temperature Effect on Performance of Different Solar Cell Technologies. *J. Ecol. Eng.* **2019**, *20*, 249–254. [CrossRef]
71. Egegik, Alaska Wind Power Feasibility Study. Available online: https://www.v3energy.com/wp-content/uploads/2017/08/Egegik-Wind-Power-Feasibility-Study-rev.-1.pdf (accessed on 1 February 2022).
72. Nurunnabi, M.; Roy, N.K.; Hossain, E.; Pota, H.R. Size Optimization and Sensitivity Analysis of Hyrbid Wind/PV Micro-Grids—A Case Study for Bangladesh. *IEEE Access* **2019**, *7*, 150120–150140. [CrossRef]
73. Lopez, R.; Arcos, T.; Sevil, J.; Agustín, J. Comparison of Lead-Acid and Li-Ion Batteries Lifetime Prediction Models in Stand-Alone Photovoltaic Systems. *Appl. Sci.* **2021**, *11*, 1099. [CrossRef]
74. Worldwide Power Products. How Long Do Diesel Generators Last? Available online: https://www.wpowerproducts.com/news/diesel-engine-life-expectancy/ (accessed on 1 February 2022).
75. Kuwait Diesel Prices. Available online: https://www.globalpetrolprices.com/Kuwait/diesel_prices/ (accessed on 1 February 2022).
76. Barley, C.; Winn, C. Optimal Dispatch Strategy in remote Hybrid Power Systems. *Sol. Energy* **1996**, *58*, 165–179. [CrossRef]
77. HOMER Pro. How HOMER Calculates Emissions. Available online: https://www.homerenergy.com/products/pro/docs/latest/how_homer_calculates_emissions.html (accessed on 1 February 2022).
78. HOMER Energy. Emission Calculation. Available online: https://homerenergy.force.com/supportcenter/s/article/emission-calculation (accessed on 1 February 2022).
79. Alsharif, M.H.; Kelechi, A.H.; Kim, J.; Kim, J.H. Energy Efficiency and Coverage Trade-off in 5G for Eco-Friendly and Sustainable Cellular Networks. *Symmetry* **2019**, *11*, 408. [CrossRef]
80. Combined Dispatch versus Cycle Charging and Load Following. Available online: https://www.homerenergy.com/products/pro/docs/latest/combined-dispatch.html (accessed on 1 February 2022).
81. Gupta, N. A Review on the Inclusion of Wind Generation in Power System Studies. *Renew. Sustain. Energy Rev.* **2016**, *59*, 530–543. [CrossRef]
82. Sanchez-Carbajal, S. Optimum Array Spacing in Grid-Connected Photovoltaic Systems Considering Technical and Economic Factors. *Int. J. Photoenergy* **2019**, *2019*, 1486749. [CrossRef]
83. FOLSOM LABS. Modeling 101—Performance Modeliwg Overview—Row-to-Row Spacing and Ground Coverage Ratio. Available online: https://www.folsomlabs.com/modeling (accessed on 1 February 2022).
84. Azar, A.T.; Kamal, N.A. *Design, Analysis, and Applications of Renewable Energy Systems*; Academic Press: London, UK, 2021.